

ESSENTIAL SOLAR NEUTRINOS

C. Giunti & M. Laveder

31 January 2003

Neutrino Unbound

<http://www.to.infn.it/~giunti/NU>

hep-ph/0301276

arXiv:hep-ph/0301276v1 31 Jan 2003

Contents

Contents	2
1 Standard Solar Model	3
2 Solar Neutrino Bibliography	4
3 Homestake	7
4 Gallium Experiments: SAGE, GALLEX, GNO	8
5 SAGE: Soviet-American Gallium Experiment	8
6 GALLEX: GALLium EXperiment	9
7 GNO: Gallium Neutrino Observatory	9
8 Kamiokande	10
9 Super-Kamiokande	10
10 SNO: Sudbury Neutrino Observatory	12
11 Main characteristics of solar ν data	14
12 Solar neutrino transitions	15
13 Two-neutrino oscillations in vacuum and matter	16
14 Fits of current solar neutrino data	21
15 $\nu_e \rightarrow \nu_\mu, \nu_\tau$ allowed regions from Ref. [39]	22
16 $\nu_e \rightarrow \nu_\mu, \nu_\tau$ allowed regions from Ref. [86]	23
17 $\nu_e \rightarrow \nu_\mu, \nu_\tau$ allowed regions from Ref. [80]	24
18 KamLAND \Rightarrow LMA	25
19 Fits of reactor + solar neutrino data	26
20 Allowed reactor + solar region from Ref. [88]	27
21 Allowed reactor + solar region from Ref. [132]	28
22 Allowed reactor + solar region from Ref. [40]	29
23 Allowed reactor + solar region from Ref. [79]	30
Bibliography	31

1 Standard Solar Model

Current Standard Solar Model (SSM): BP2000 [46, 28]

pp and CNO cycles: $4p + 2e^- \rightarrow {}^4\text{He} + 2\nu_e + 26.731 \text{ MeV}$

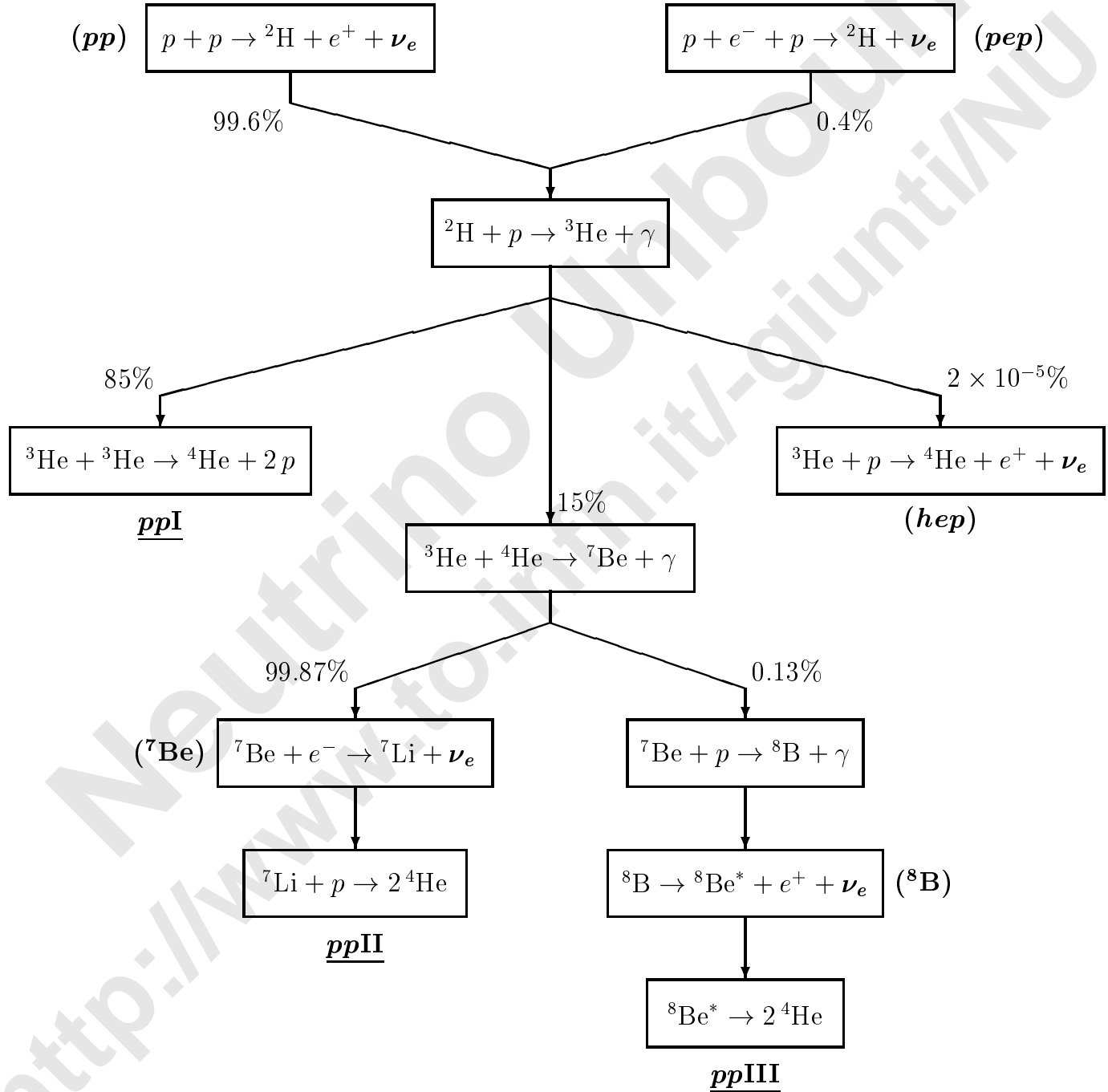
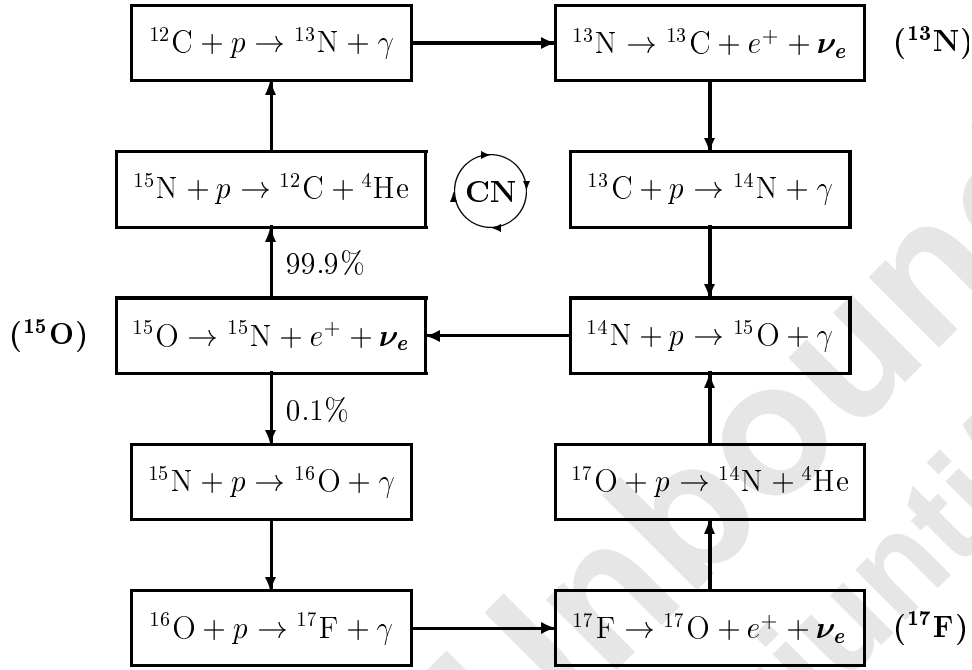


Figure 1: *pp* cycle.



Luminosity	$\mathcal{L}_\odot = (2.400 \pm 0.005) \times 10^{39} \text{ MeV s}^{-1}$
Radius	$\mathcal{R}_\odot = 6.961 \times 10^{10} \text{ cm}$
Mass	$\mathcal{M}_\odot = (1.989 \pm 0.003) \times 10^{33} \text{ g}$
Astronomical Unit	1a.u. = $1.496 \times 10^{13} \text{ cm}$
Solar Constant	$K_\odot \equiv \mathcal{L}_\odot / 4\pi(1\text{a.u.})^2 = 8.534 \times 10^{11} \text{ MeV cm}^{-2} \text{ s}^{-1}$

Table 1: Fundamental characteristics of the Sun and Sun-Earth system [101]. One astronomical unit is the mean sun-earth distance. The solar constant K_\odot is the mean solar photon flux on the Earth.

$$\text{Luminosity Constraint [33]: } \sum_r \alpha_r \Phi_r = K_\odot \quad (r = pp, pep, hep, {}^7\text{Be}, {}^8\text{B}, {}^{13}\text{N}, {}^{15}\text{O}, {}^{17}\text{F}) \quad (1)$$

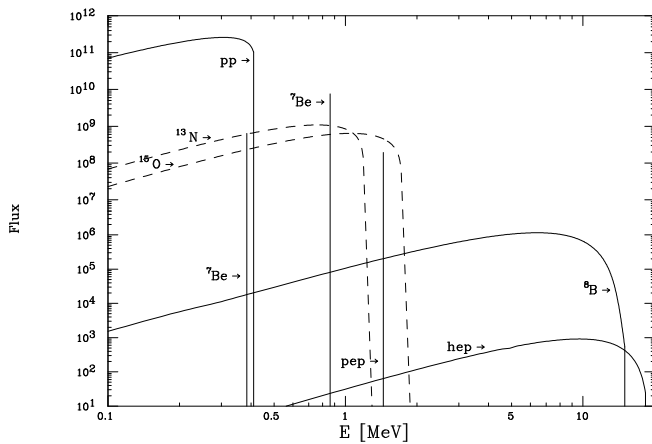
2 Solar Neutrino Bibliography

Books: [153, 30]

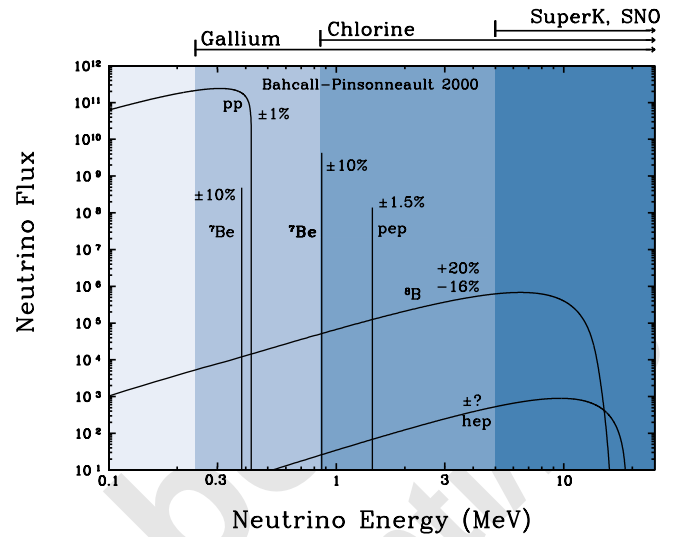
Reviews: [70, 163, 136]

Bahcall's Standard Solar Models: [29, 41, 47, 44, 45, 34, 46, 28]

Detection cross sections: [30, 37, 32, 28, 143, 69, 138, 20]



(a) Figure from Ref. [70].



(b) Figure from Ref. [28].

Figure 3: Energy spectra of neutrino fluxes from the pp and CNO chains, as predicted by the Standard Solar Model. For continuous sources, the differential flux is in $\text{cm}^{-2} \text{s}^{-1} \text{MeV}^{-1}$. For the lines, the flux is in $\text{cm}^{-2} \text{s}^{-1}$. The percentages in Fig. 3(b) indicate the uncertainties on the values of the fluxes.

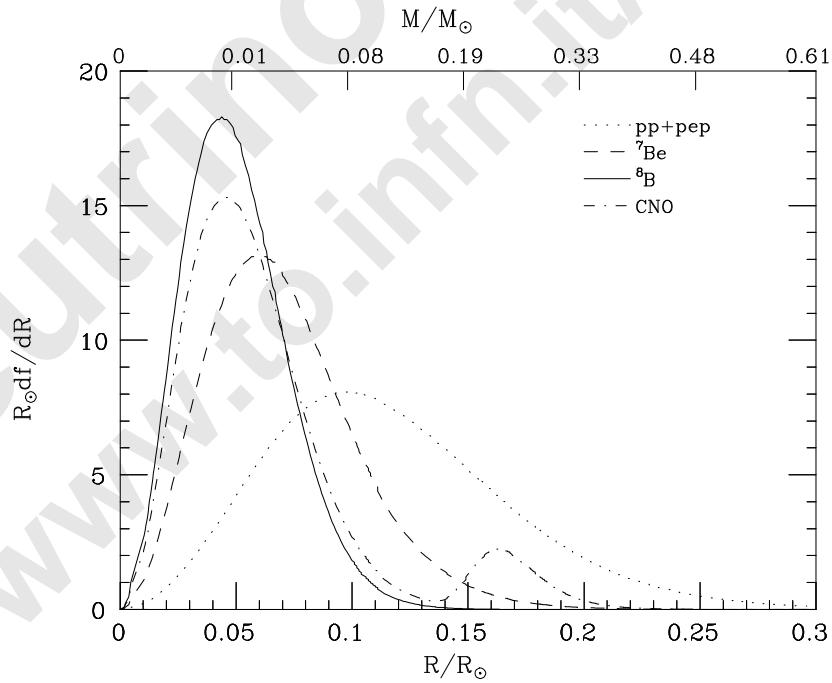


Figure 4: Differential fraction df/dR of produced neutrinos as a function of radius R , normalized to the solar radius R_\odot . Figure from Ref. [70].

Source r	Reaction	$\langle E \rangle_r$ (MeV)	E_r^{\max} (MeV)	α_r (MeV)
pp	$p + p \rightarrow d + e^+ + \nu_e$	0.2668	0.423 ± 0.03	13.0987
pep	$p + e^- + p \rightarrow d + \nu_e$	1.445	1.445	11.9193
hep	${}^3\text{He} + p \rightarrow {}^4\text{He} + e^+ + \nu_e$	9.628	18.778	3.7370
${}^7\text{Be}$	$e^- + {}^7\text{Be} \rightarrow {}^7\text{Li} + \nu_e$	0.3855 0.8631	0.3855 0.8631	12.6008
${}^8\text{B}$	${}^8\text{B} \rightarrow {}^8\text{Be}^* + e^+ + \nu_e$	6.735 ± 0.036	~ 15	6.6305
${}^{13}\text{N}$	${}^{13}\text{N} \rightarrow {}^{13}\text{C} + e^+ + \nu_e$	0.7063	1.1982 ± 0.0003	3.4577
${}^{15}\text{O}$	${}^{15}\text{O} \rightarrow {}^{15}\text{N} + e^+ + \nu_e$	0.9964	1.7317 ± 0.0005	21.5706
${}^{17}\text{F}$	${}^{17}\text{F} \rightarrow {}^{17}\text{O} + e^+ + \nu_e$	0.9977	1.7364 ± 0.0003	2.363

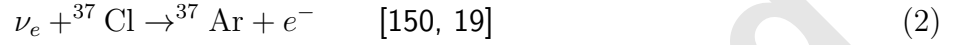
Table 2: Sources of solar neutrinos [30, 37, 32, 31]. For each reaction r , $\langle E \rangle_r$ is the average neutrino energy, E_r^{\max} is the maximum neutrino energy and α_r is the average thermal energy released together with a neutrino from the source r [33], that enters in the luminosity constraint (1).

Source r	Flux Φ_r ($\text{cm}^{-2} \text{s}^{-1}$)	$\langle \sigma_{\text{Cl}} \rangle_r$ (10^{-44}cm^2)	$S_{\text{Cl}}^{(r)}$ (SNU)	$\langle \sigma_{\text{Ga}} \rangle_r$ (10^{-44}cm^2)	$S_{\text{Ga}}^{(r)}$ (SNU)
pp	$5.95 \times 10^{10} (1 \pm 0.01)$	–	–	0.117 ± 0.003	69.7
pep	$1.40 \times 10^8 (1 \pm 0.015)$	0.16	0.22	$2.04^{+0.35}_{-0.14}$	2.8
hep	9.3×10^3	390	0.04	714^{+228}_{-114}	0.1
${}^7\text{Be}$	$4.77 \times 10^9 (1 \pm 0.10)$	0.024	1.15	$0.717^{+0.050}_{-0.021}$	34.2
${}^8\text{B}$	$5.05 \times 10^6 (1^{+0.20}_{-0.16})$	114 ± 11	5.76	240^{+77}_{-36}	12.1
${}^{13}\text{N}$	$5.48 \times 10^8 (1^{+0.21}_{-0.17})$	0.017	0.09	$0.604^{+0.036}_{-0.018}$	3.4
${}^{15}\text{O}$	$4.80 \times 10^8 (1^{+0.25}_{-0.19})$	0.068 ± 0.001	0.33	$1.137^{+0.136}_{-0.057}$	5.5
${}^{17}\text{F}$	$5.63 \times 10^6 (1 \pm 0.25)$	0.069	0.0	$1.139^{+0.137}_{-0.057}$	0.1
Total	6.54×10^{10}		$7.6^{+1.3}_{-1.1}$		128^{+9}_{-7}

Table 3: BP2000 Standard Solar Model [46] neutrino fluxes, average neutrino cross sections [30, 37, 32] and BP2000 SSM predictions for the neutrino capture rates [46] in the chlorine (Cl) Homestake experiment and in the gallium (Ga) GALLEX, SAGE and GNO experiments.

3 Homestake

radiochemical experiment [29, 77]



Homestake Gold Mine (Lead, South Dakota, USA)

1478 m deep, 4200 m.w.e. $\Rightarrow \Phi_\mu \simeq 4 \text{ m}^{-2} \text{ day}^{-1}$

steel tank, 6.1 m diameter, 14.6 m long (6×10^5 liters)

615 tons of tetrachloroethylene (C_2Cl_4), 2.16×10^{30} atoms of ${}^{37}\text{Cl}$ (133 tons)

energy threshold: $E_{\text{th}}^{\text{Cl}} = 0.814 \text{ MeV} \Rightarrow {}^8\text{B}, {}^7\text{Be}, \text{pep}, \text{hep}$

data taking: 1970–1994, 108 extractions [75] – history: [36, 35]

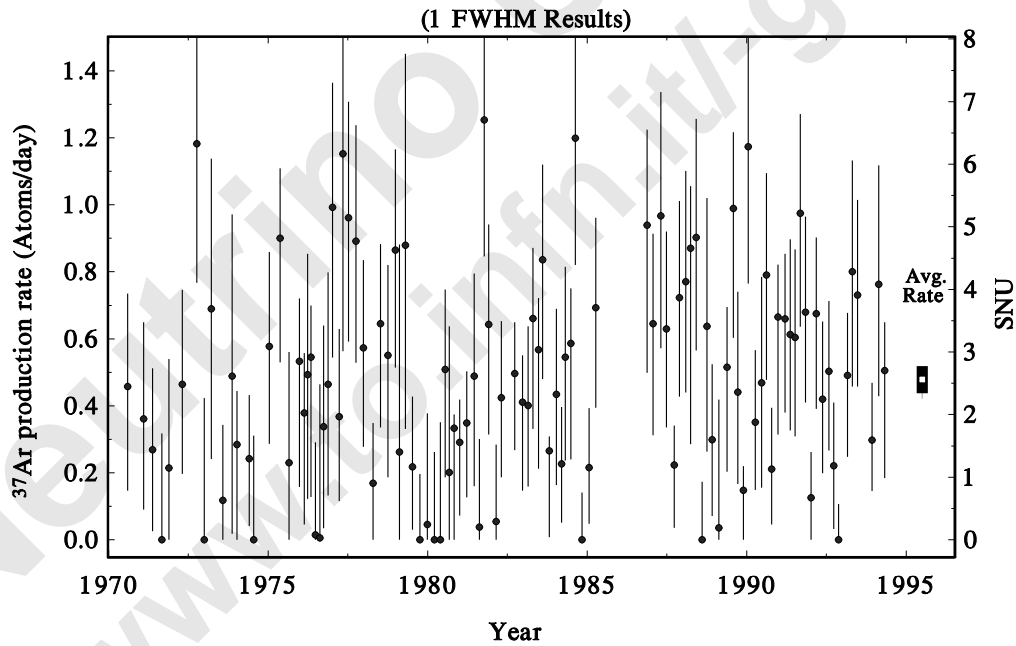


Figure 5: Results of the 108 individual solar neutrino observations made with the Homestake chlorine detector. The production rate of ${}^{37}\text{Ar}$ shown has already had all known sources of nonsolar ${}^{37}\text{Ar}$ production subtracted from it. The errors shown for individual measurements are statistical errors only and are significantly non-Gaussian for results near zero. The error shown for the cumulative result is the combination of the statistical and systematic errors in quadrature. Figure from Ref. [75].

$$R_{\text{Cl}}^{\text{exp}} = 2.56 \pm 0.16 \pm 0.16 \text{ SNU} = 2.56 \pm 0.23 \text{ SNU} \quad [75] \quad (3)$$

$$R_{\text{Cl}}^{\text{SSM}} = 7.6_{-1.1}^{+1.3} \text{ SNU} \quad [46, 28] \quad (4)$$

4 Gallium Experiments: SAGE, GALLEX, GNO

radiochemical experiments



threshold: $E_{\text{th}}^{\text{Ga}} = 0.233 \text{ MeV} \Rightarrow$ all ν fluxes (pp , ${}^7\text{Be}$, ${}^8\text{B}$, pep , hep , ${}^{13}\text{N}$, ${}^{15}\text{O}$, ${}^{17}\text{F}$)

$$\text{SAGE} + \text{GALLEX} + \text{GNO} \Rightarrow R_{\text{Ga}}^{\text{exp}} = 72.4 \pm 4.7 \text{ SNU} \quad (6)$$

$$\text{Standard Solar Model} \Rightarrow R_{\text{Ga}}^{\text{SSM}} = 128_{-7}^{+9} \text{ SNU} \quad [46, 28] \quad (7)$$

5 SAGE: Soviet-American Gallium Experiment

Baksan Neutrino Observatory, northern Caucasus, 3.5 km from entrance of horizontal adit

50 tons of metallic ${}^{71}\text{Ga}$, 2000 m deep, 4700 m.w.e. $\Rightarrow \Phi_{\mu} \simeq 2.6 \text{ m}^{-2} \text{ day}^{-1}$

data taking: 1990 – 2001, 92 runs [1, 2, 5, 6, 7]

detector test: ${}^{51}\text{Cr}$ Source ($R = 0.95_{-0.10}^{+0.11+0.06}$) [3, 4]

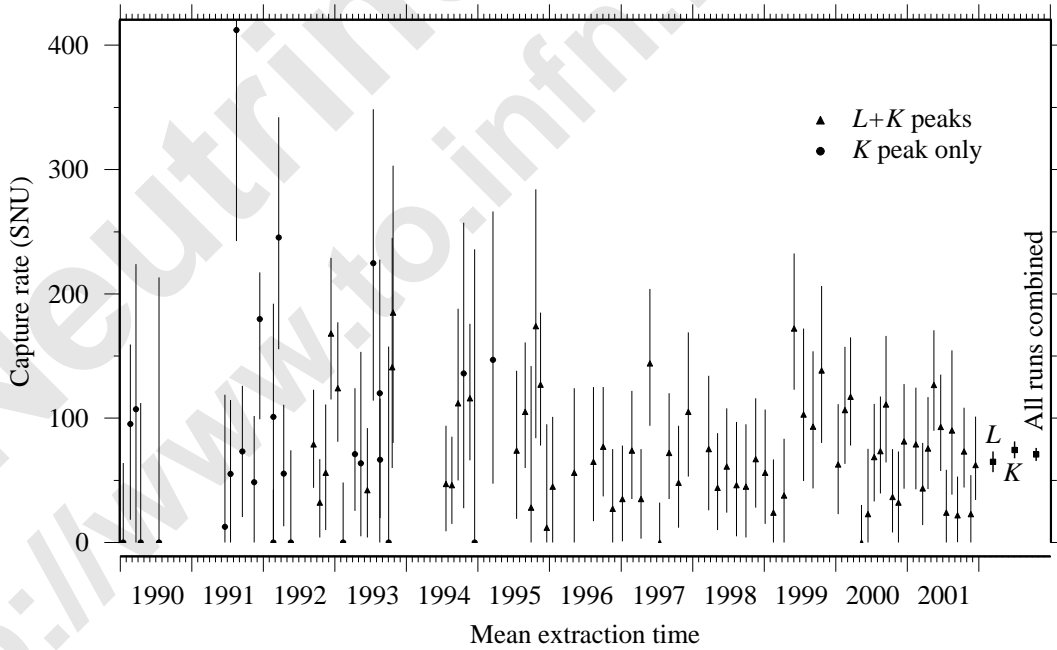


Figure 6: Capture rate for all SAGE extractions as a function of time. Error bars are statistical with 68% confidence. The combined result of all runs in the L peak, the K peak, and both L and K peaks is shown on the right side. The last 3 runs are still counting and their results are preliminary. Figure from Ref. [7].

$$R_{\text{Ga}}^{\text{SAGE}} = 70.8_{-5.2-3.2}^{+5.3+3.7} \text{ SNU} = 70.8_{-6.1}^{+6.5} \text{ SNU} \quad [7] \quad (8)$$

6 GALLEX: GALLium EXperiment

Gran Sasso Underground Laboratory, Italy, overhead shielding: 3300 m.w.e.

30.3 tons of gallium in 101 tons of gallium chloride ($\text{GaCl}_3\text{-HCl}$) solution

data taking: May 1991 – Jan 1997, 65 runs [21, 22, 23, 25, 105, 108]

detector tests: ^{51}Cr Source ($R = 0.93 \pm 0.08$) [24, 106], ^{71}As Test [107]

$$R_{\text{Ga}}^{\text{GALLEX}} = 77.5 \pm 6.2^{+4.3}_{-4.7} \text{SNU} = 77.5^{+7.6}_{-7.8} \text{SNU} \quad [108] \quad (9)$$

7 GNO: Gallium Neutrino Observatory

successor of GALLEX, GNO30: 30.3 tons of gallium

data taking: May 1998 – Jan 2000, 19 runs [18]

$$R_{\text{Ga}}^{\text{GNO}} = 65.8^{+10.2+3.4}_{-9.6-3.6} \text{SNU} = 65.8^{+10.7}_{-10.2} \text{SNU} \quad [18] \quad (10)$$

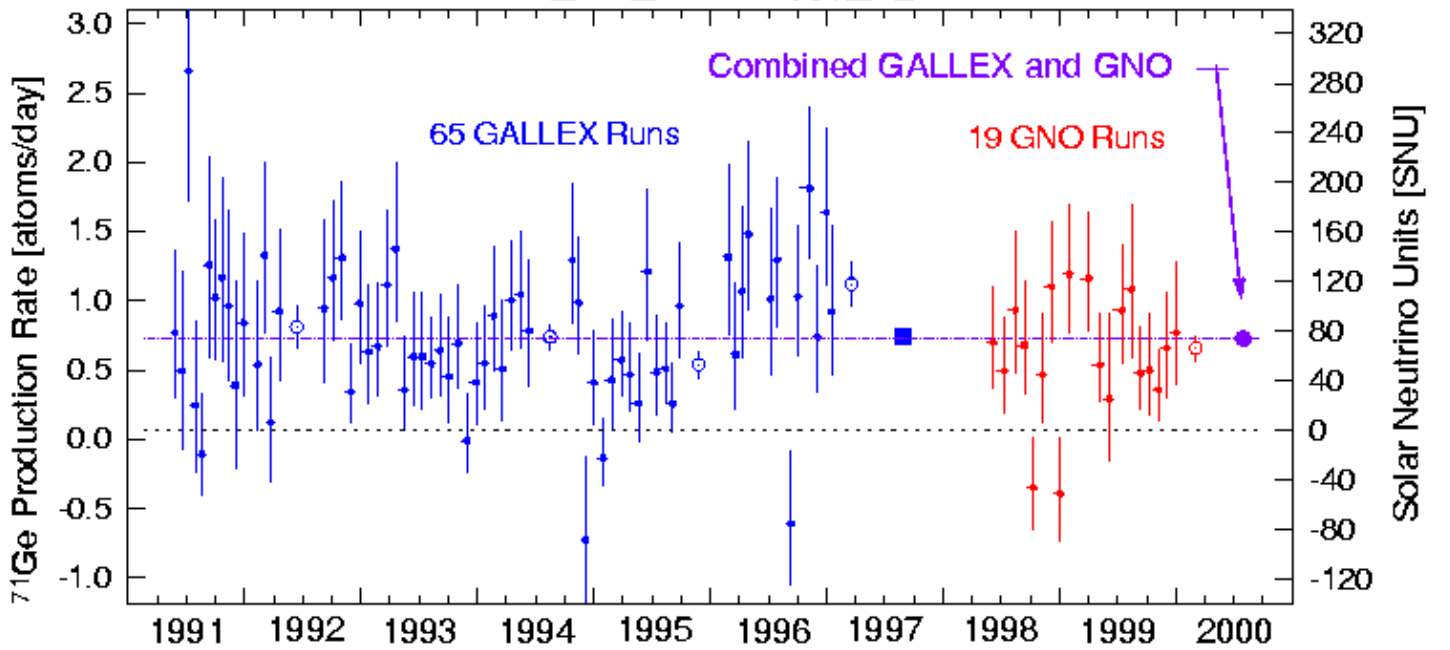


Figure 7: GNO and GALLEX single run results. Error bars are statistical only. Open dots represent group mean values; the bold square represents the global result of GALLEX; the bold solid dot represents the global result of GNO and Gallex. Figure from Ref. [18].

$$\text{GALLEX} + \text{GNO} \implies R_{\text{Ga}}^{\text{GALLEX+GNO}} = 74.1 \pm 5.4^{+4.0}_{-4.2} \text{SNU} = 74.1^{+6.7}_{-6.8} \text{SNU} \quad [18] \quad (11)$$

8 Kamiokande

real-time water Cherenkov detector $\nu + e^- \rightarrow \nu + e^-$ [117, 159]

Sensitive to ν_e, ν_μ, ν_τ , but $\sigma(\nu_e) \simeq 6\sigma(\nu_{\mu,\tau})$

Kamioka mine (200 km west of Tokyo), 1000 m underground, 2700 m.w.e.

3000 tons of water, 680 tons fiducial volume, 948 PMTs

threshold: $E_{\text{th}}^{\text{Kam}} \simeq 6.75 \text{ MeV} \Rightarrow {}^8\text{B}, \text{ hep}$

data taking: Jan 1987 – Feb 1995 (2079 days) [110, 111, 112, 114, 113, 94]

$$\Phi_{\nu_e}^{\text{Kam}} = 2.82_{-0.24}^{+0.25} \pm 0.27 \times 10^6 \text{ cm}^{-2}\text{s}^{-1} = 2.82 \pm 0.37 \times 10^6 \text{ cm}^{-2}\text{s}^{-1} \quad [94] \quad (12)$$

$$\text{Standard Solar Model} \Rightarrow \Phi_{\nu_e}^{{}^8\text{B}} = 5.05_{-0.81}^{+1.01} \times 10^6 \text{ cm}^{-2}\text{s}^{-1} \quad [46, 28] \quad (13)$$

9 Super-Kamiokande

successor of Kamiokande, 50 ktons of water, 22.5 ktons fiducial volume, 11146 PMTs

threshold: $E_{\text{th}}^{\text{Kam}} \simeq 4.75 \text{ MeV} \Rightarrow {}^8\text{B}, \text{ hep}$

data taking: 1996 – 2001 (1496 days) [95, 96, 97, 92, 91, 93]

$$\Phi_{\nu_e}^{\text{SK}} = 2.348 \pm 0.025_{-0.061}^{+0.071} \times 10^6 \text{ cm}^{-2}\text{s}^{-1} = 2.348_{-0.066}^{+0.075} \times 10^6 \text{ cm}^{-2}\text{s}^{-1} \quad [93] \quad (14)$$

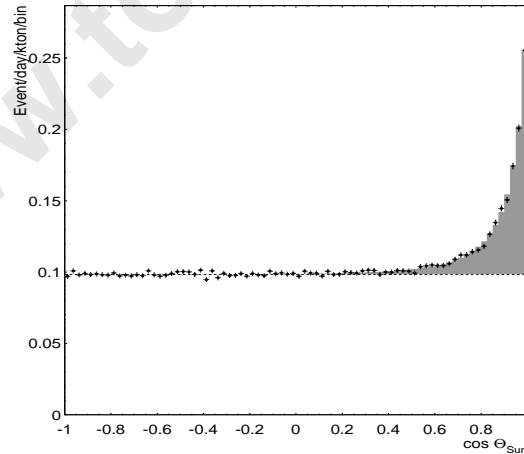


Figure 8: Super-Kamiokande $\cos \theta_{\text{sun}}$ distribution. The points represent observed data. The histogram shows the best-fit signal (shaded) plus background. The horizontal dashed line shows the estimated background. Figure from Ref. [155].

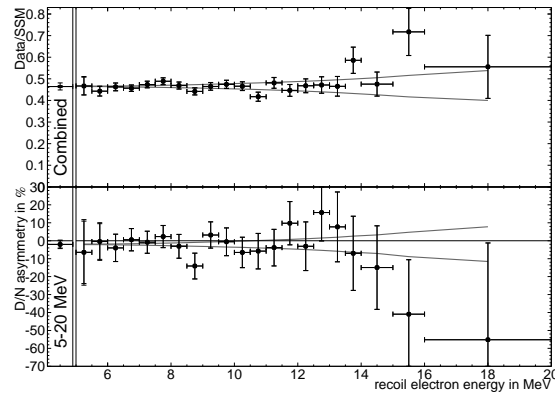


Figure 9: Super-Kamiokande energy spectrum normalized to BP2000 SSM [155].

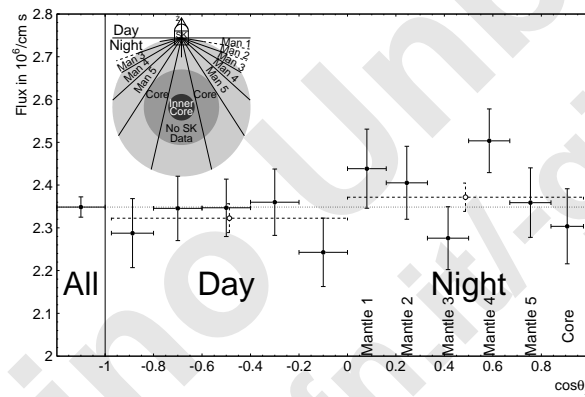


Figure 10: Solar zenith angle (θ_z) dependence of Super-Kamiokande data [155].

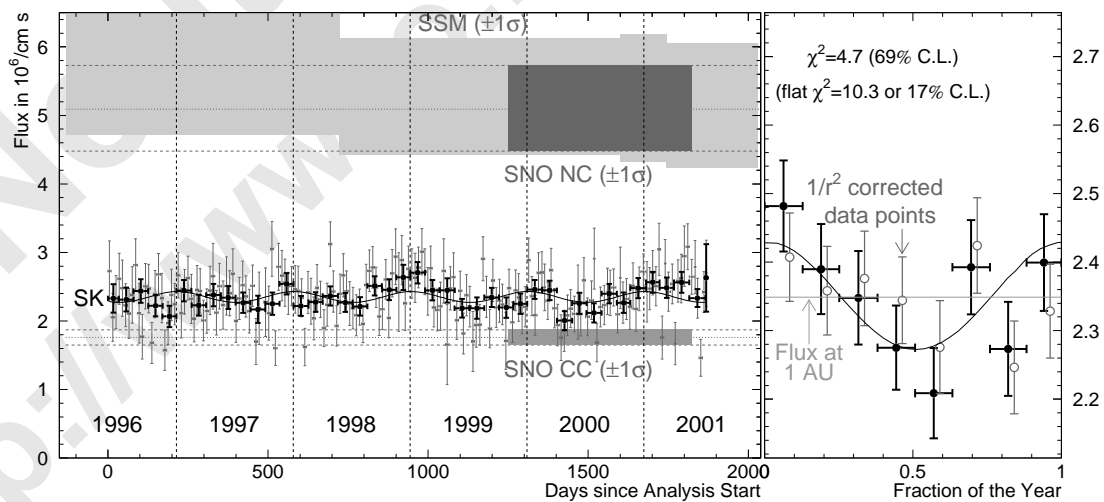


Figure 11: Time variation of the Super-Kamiokande data. The gray data points are measured every 10 days, the black data points every 1.5 months. The black line indicates the expected annual 7% flux variation. The right-hand panel combines the 1.5 month bins to search for yearly variations. The gray data points (open circles) are obtained from the black data points by subtracting the expected 7% variation. Figure from Ref. [155].

10 SNO: Sudbury Neutrino Observatory

real-time heavy-water Cherenkov detector

Creighton mine (INCO Ltd.), Sudbury, Ontario, Canada

1 kton of D₂O, 9456 20-cm PMTs

2073 m underground, 6010 m.w.e.

$$\left. \begin{array}{l} \text{CC threshold: } E_{\text{th}}^{\text{SNO}}(\text{CC}) \simeq 8.2 \text{ MeV} \\ \text{NC threshold: } E_{\text{th}}^{\text{SNO}}(\text{NC}) \simeq 2.2 \text{ MeV} \\ \text{ES threshold: } E_{\text{th}}^{\text{SNO}}(\text{ES}) \simeq 7.0 \text{ MeV} \end{array} \right\} \Rightarrow {}^8\text{B, hep}$$

data taking: 1999 – 2002 (306.4 days) [9, 10, 11]

$$\Phi_{\text{CC}}^{\text{SNO}} = 1.76_{-0.05}^{+0.06} \pm 0.09 \times 10^6 \text{ cm}^{-2}\text{s}^{-1} = 1.76_{-0.10}^{+0.11} \times 10^6 \text{ cm}^{-2}\text{s}^{-1} \quad [10] \quad (15)$$

$$\Phi_{\text{NC}}^{\text{SNO}} = 5.09_{-0.43}^{+0.44+0.46} \times 10^6 \text{ cm}^{-2}\text{s}^{-1} = 5.09_{-0.61}^{+0.64} \times 10^6 \text{ cm}^{-2}\text{s}^{-1} \quad [10] \quad (16)$$

$$\Phi_{\text{ES}}^{\text{SNO}} = 2.39_{-0.23}^{+0.24} \pm 0.12 \times 10^6 \text{ cm}^{-2}\text{s}^{-1} = 2.39_{-0.26}^{+0.27} \times 10^6 \text{ cm}^{-2}\text{s}^{-1} \quad [10] \quad (17)$$

$$\Phi_{\nu_e}^{\text{SNO}} = 1.76 \pm 0.05 \pm 0.09 \times 10^6 \text{ cm}^{-2}\text{s}^{-1} = 1.76 \pm 0.10 \times 10^6 \text{ cm}^{-2}\text{s}^{-1} \quad [10] \quad (18)$$

$$\Phi_{\nu_{\mu,\tau}}^{\text{SNO}} = 3.41 \pm 0.45_{-0.45}^{+0.48} \times 10^6 \text{ cm}^{-2}\text{s}^{-1} = 3.41_{-0.64}^{+0.66} \times 10^6 \text{ cm}^{-2}\text{s}^{-1} \quad [10] \quad (19)$$

5.3 σ evidence of $\nu_e \rightarrow \nu_{\mu,\tau}$ transitions

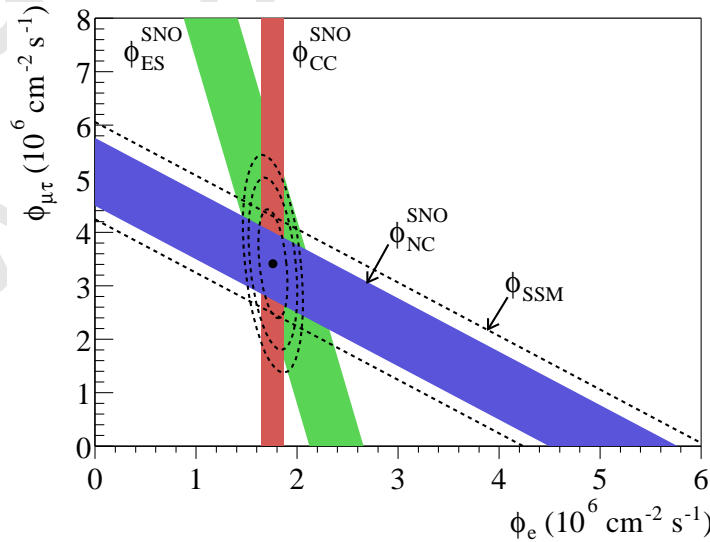
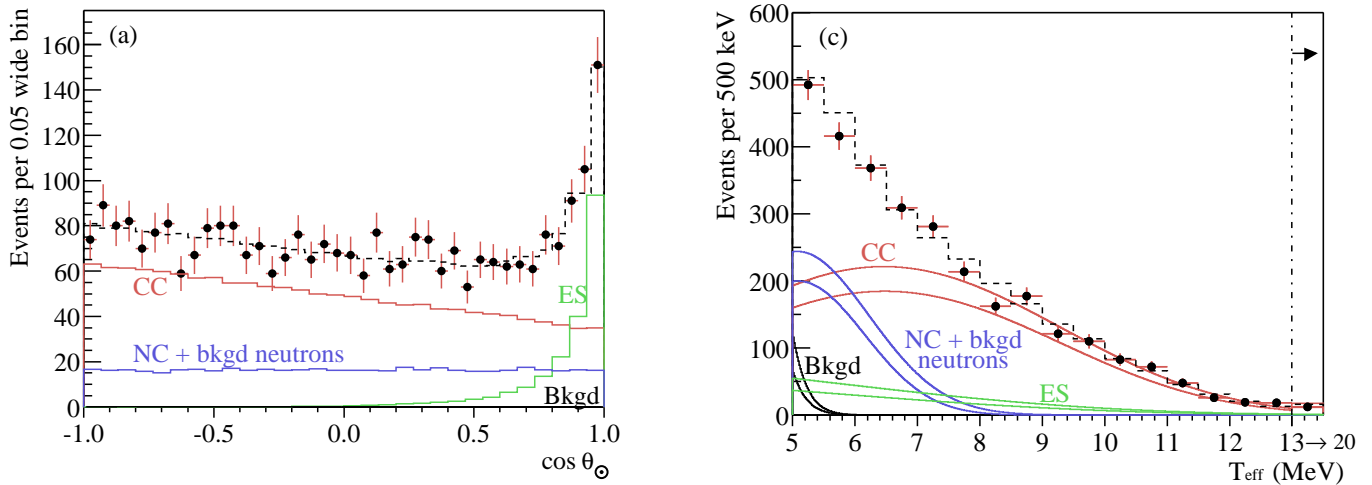


Figure 12: Flux of ν_{μ} and ν_{τ} vs flux of ν_e in the ${}^8\text{B}$ energy range deduced from the three neutrino reactions in SNO. The diagonal bands show the total BP2000 ${}^8\text{B}$ flux [46] (dashed lines) and that measured with the NC reaction in SNO (solid band). The intercepts of these bands with the axes represent the $\pm 1\sigma$ errors. The bands intersect at the fit values for $\phi_e \equiv \Phi_{\nu_e}$ and $\phi_{\mu\tau} \equiv \Phi_{\nu_{\mu,\tau}}$. Figure from Ref. [10].



(a) Solar zenith angle (θ_{\odot}) dependence of SNO data. ES: $\cos \theta_{\odot} \simeq 1$. CC: $\sigma \propto 1 - 0.340 \cos \theta_{\odot}$. NC: isotropic.

(b) SNO electron kinetic energy spectrum.

Figure 13: Figures taken from Ref. [10].

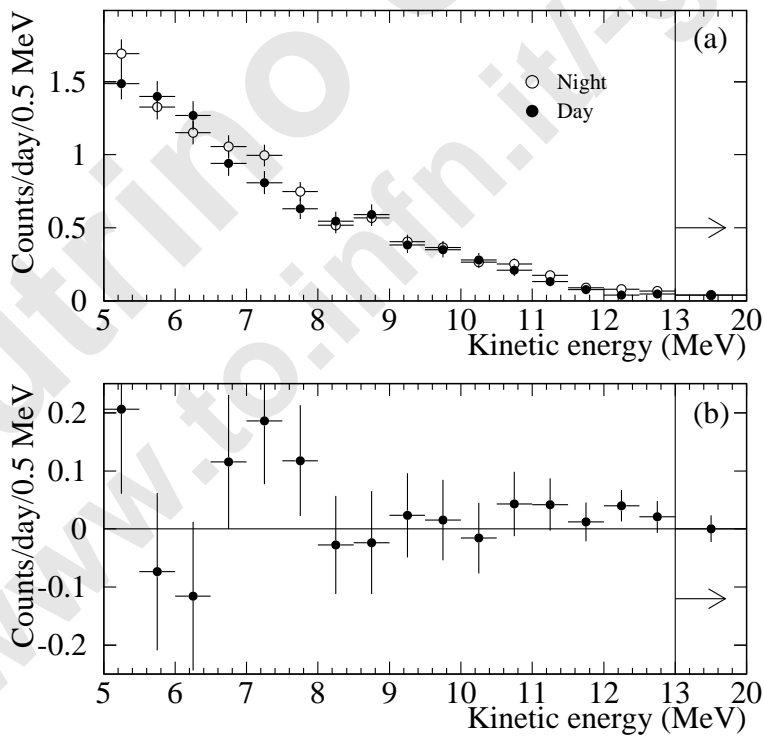


Figure 14: (a) SNO day and night energy spectra. (b) Night - day difference between the spectra (night rate = 9.79 ± 0.24 events/day, day rate = 9.23 ± 0.27 events/day). Figure from Ref. [11].

11 Main characteristics of solar ν data

Experiment	Reaction	E_{th} (MeV)	ν Flux Sensitivity	Operating Time	$\frac{R^{\text{exp}}}{R^{\text{BP2000}}}$
SAGE	$\nu_e + {}^{71}\text{Ga} \rightarrow {}^{71}\text{Ge} + e^-$	0.233	$pp, {}^7\text{Be}, {}^8\text{B},$ $pep, hep,$ ${}^{13}\text{N}, {}^{15}\text{O}, {}^{17}\text{F}$	1990 – 2001	0.55 ± 0.05 [7]
GALLEX				1991 – 1997	0.61 ± 0.06 [108]
GNO				1998 – 2000	0.51 ± 0.08 [18]
Homestake	$\nu_e + {}^{37}\text{Cl} \rightarrow {}^{37}\text{Ar} + e^-$	0.814	${}^7\text{Be}, {}^8\text{B},$ $pep, hep,$ ${}^{13}\text{N}, {}^{15}\text{O}, {}^{17}\text{F}$	1970 – 1994	0.34 ± 0.03 [75]
Kamiokande	$\nu + e^- \rightarrow \nu + e^-$	6.75	${}^8\text{B}$	1987 – 1995 2079 days	0.55 ± 0.08 [94]
Super-Kam.		4.75		1996 – 2001 1496 days	0.465 ± 0.015 [93]
SNO	$\nu_e + d \rightarrow p + p + e^-$	6.9	${}^8\text{B}$	1999 – 2002 306.4 days	0.35 ± 0.02 [10]
	$\nu + d \rightarrow p + n + \nu$	2.2			1.01 ± 0.13 [10]
	$\nu + e^- \rightarrow \nu + e^-$	5.2			0.47 ± 0.05 [10]

$$\text{Super-Kamiokande: } \Phi_{hep} < 7.9 \Phi_{hep}^{\text{SSM}} \quad (90\% \text{ CL}) \quad [155] \quad (20)$$

$$\text{Super-Kamiokande energy spectrum: no distortion [155]} \quad (21)$$

$$\text{SNO energy spectrum: no distortion [11]} \quad (22)$$

$$\text{Super-Kamiokande time variations: none [155]} \quad (23)$$

$$\text{Super-Kamiokande night-day asymmetry: } \mathcal{A}_{\text{ND}}^{\text{SK}} = 0.021 \pm 0.024 \quad [93] \quad (24)$$

$$\text{SNO night-day asymmetry: } \mathcal{A}_{\text{ND}}^{\text{SNO}} = 0.070 \pm 0.051 \quad [11] \quad (25)$$

12 Solar neutrino transitions

Books: [68, 30, 116, 137]

Reviews: [66, 65, 135, 123, 152, 64, 84, 62, 63, 99]

Vacuum Oscillations: [151, 100, 57, 8, 119, 120]

MSW Effect: [162, 58, 133, 134, 61, 142, 144, 145, 118, 146, 124]

Regeneration in Earth: [135, 76, 50, 51, 52, 128, 129, 147, 12, 81, 72, 73, 102]

Quasi-Vacuum Oscillations: [89, 87, 90, 127]

Three-Neutrino Mixing: [121, 122, 158, 148, 154]

Four-Neutrino Mixing: [82, 98]

Flavor-Changing Neutral Currents: [162, 160, 103, 104]

Spin-Flavor Precession: [74, 161, 139, 141, 140, 13, 126, 14, 15]

Neutrino Unbound
<http://www.to.infn.it/~giunti/NU>

13 Two-neutrino oscillations in vacuum and matter

$$\text{mixing: } \nu_e = \cos\vartheta\nu_1 + \sin\vartheta\nu_2, \quad \nu_f = -\sin\vartheta\nu_1 + \cos\vartheta\nu_2 \quad (f = \mu, \tau, s) \quad (26)$$

$$\text{transition probability in vacuum: } P_{\nu_e \rightarrow \nu_f}(R) = \sin^2 2\vartheta \sin^2 \left(\frac{\Delta m^2 R}{4E} \right) \quad (27)$$

$$R = \text{distance from the center of the Sun, } \Delta m^2 \equiv m_2^2 - m_1^2 \quad (28)$$

$$\text{evolution in matter: } i \frac{d}{dR} \begin{pmatrix} \phi_{\nu_e}(R) \\ \phi_{\nu_f}(R) \end{pmatrix} = \frac{1}{4E} \begin{pmatrix} -\Delta m^2 \cos 2\vartheta + 2A & \Delta m^2 \sin 2\vartheta \\ \Delta m^2 \sin 2\vartheta & \Delta m^2 \cos 2\vartheta \end{pmatrix} \begin{pmatrix} \phi_{\nu_e}(R) \\ \phi_{\nu_f}(R) \end{pmatrix} \quad (29)$$

$$\phi_{\nu_e}(0) = 1, \quad \phi_{\nu_f}(0) = 0 \implies P_{\nu_e \rightarrow \nu_f}(R) = |\phi_{\nu_f}(R)|^2 \quad (30)$$

$$A = 2EV \quad \text{with} \quad \begin{cases} V = V_{CC} = \sqrt{2}G_F N_e & \text{for } f = \mu, \tau \\ V = V_{CC} + V_{NC} = \sqrt{2}G_F (N_e - \frac{1}{2}N_n) & \text{for } f = s \end{cases} \quad (31)$$

N_e = electron number density

N_n = neutron number density

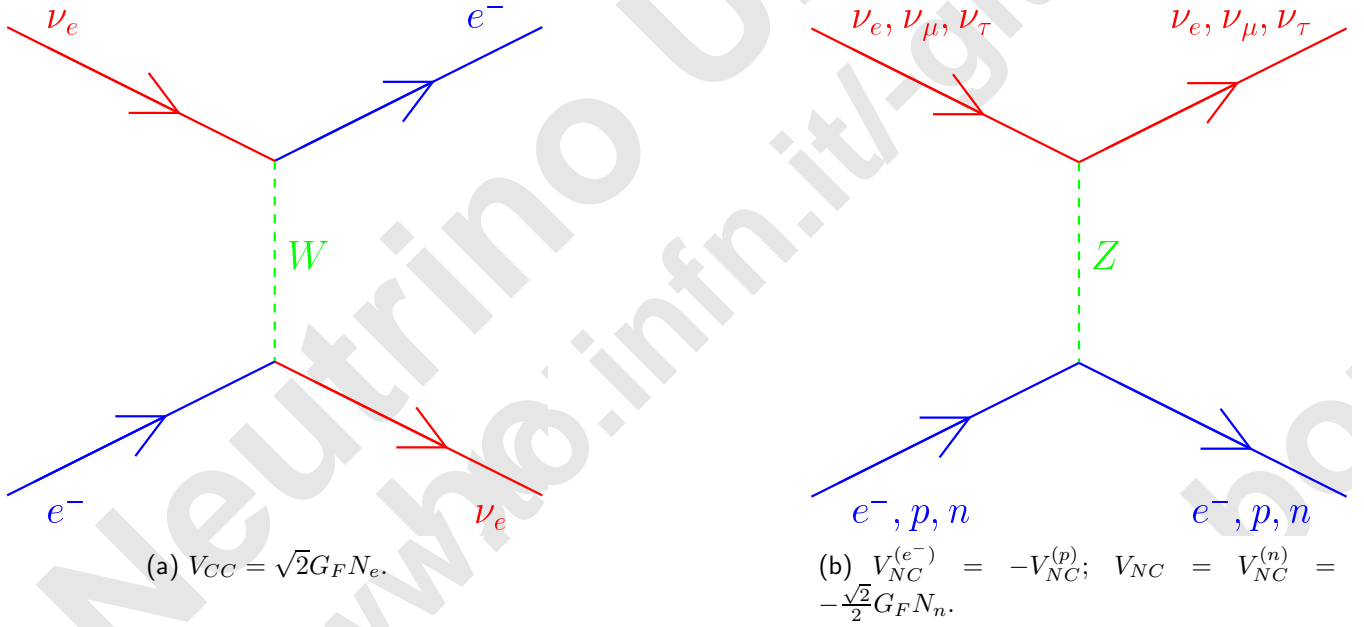


Figure 15: $V_{\nu_e} = V_{CC} + V_{NC}$; $V_{\nu_\mu} = V_{\nu_\tau} = V_{NC}$; $V_{\nu_e} - V_{\nu_{\mu,\tau}} = V_{CC} = \sqrt{2}G_F N_e$; $V_{\nu_e} - V_{\nu_s} = V_{CC} + V_{NC} = \sqrt{2}G_F (N_e - \frac{1}{2}N_n)$.

$$V = \sqrt{2}G_F N = 7.63 \times 10^{-14} \left(\frac{N}{N_A \text{ cm}^{-3}} \right) \text{ eV} \quad \text{with} \quad \begin{cases} N = N_e & \text{for } f = \mu, \tau \\ N = N_e - \frac{1}{2}N_n & \text{for } f = s \end{cases} \quad (32)$$

$$\text{effective mixing angle: } \tan 2\vartheta_M = \frac{\tan 2\vartheta}{1 - \frac{A}{\Delta m^2 \cos 2\vartheta}}, \quad \text{resonance: } A_{\text{res}} = \Delta m^2 \cos 2\vartheta \quad (33)$$

$$\text{effective squared-mass difference: } \Delta m_{M}^2 = \sqrt{(\Delta m^2 \cos 2\vartheta - A)^2 + (\Delta m^2 \sin 2\vartheta)^2} \quad (34)$$

$$\text{effective squared masses: } (m_{2,1}^M)^2 = m_1^2 + \frac{1}{2} (\Delta m^2 + A \pm \Delta m_M^2) \quad (35)$$

standard terminology for regions in the Δm^2 - $\tan^2 \vartheta$ plane:

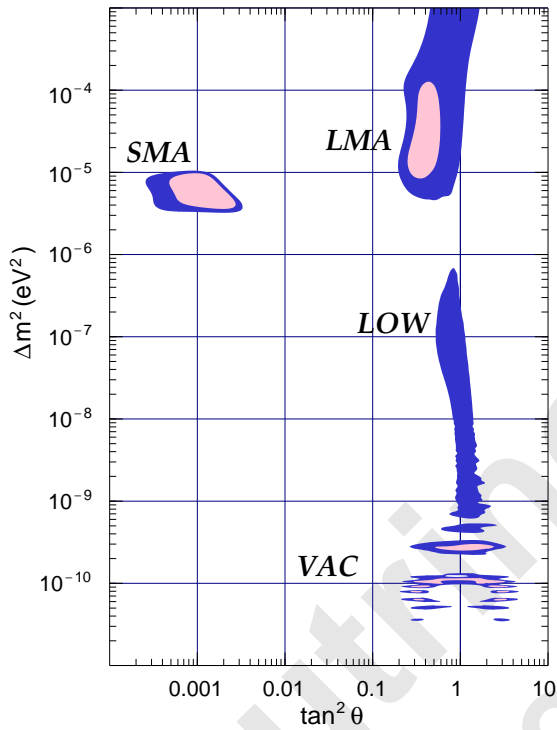
$$\text{LMA (Large Mixing Angle): } \Delta m^2 \sim 5 \times 10^{-5} \text{ eV}^2, \quad \tan^2 \vartheta \sim 0.8 \quad (36)$$

$$\text{LOW (LOW } \Delta m^2\text{): } \Delta m^2 \sim 7 \times 10^{-8} \text{ eV}^2, \quad \tan^2 \vartheta \sim 0.6 \quad (37)$$

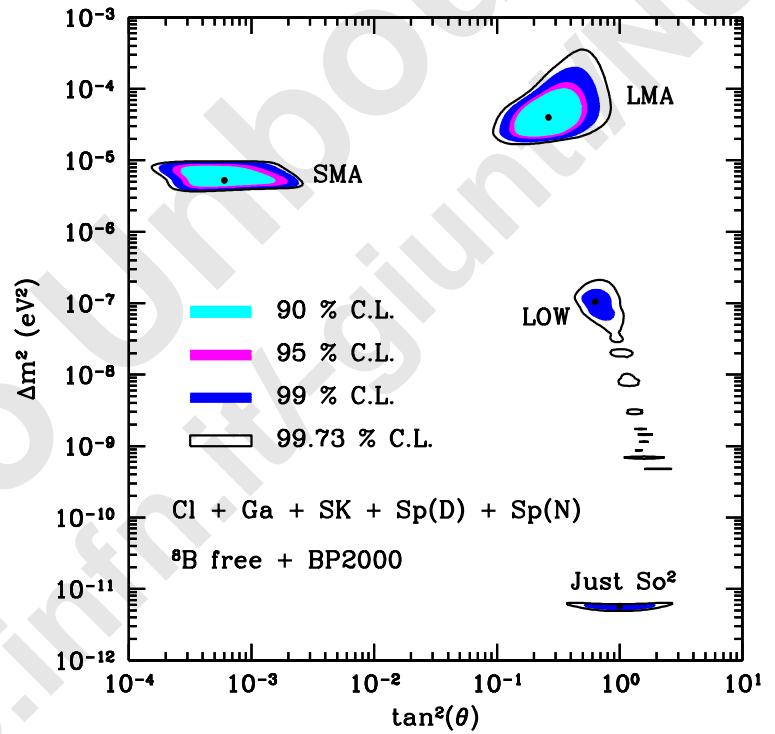
$$\text{SMA (Small Mixing Angle): } \Delta m^2 \sim 5 \times 10^{-6} \text{ eV}^2, \quad \tan^2 \vartheta \sim 10^{-3} \quad (38)$$

$$\text{QVO (Quasi-Vacuum Oscillations): } \Delta m^2 \sim 10^{-9} \text{ eV}^2, \quad \tan^2 \vartheta \sim 1 \quad (39)$$

$$\text{VAC (VACuum oscillations): } \Delta m^2 \lesssim 5 \times 10^{-10} \text{ eV}^2, \quad \tan^2 \vartheta \sim 1 \quad (40)$$



(a) Figure from Ref. [78].



(b) Figure from Ref. [43].

Figure 16: Regions in the Δm^2 - $\tan^2 \vartheta$ plane.

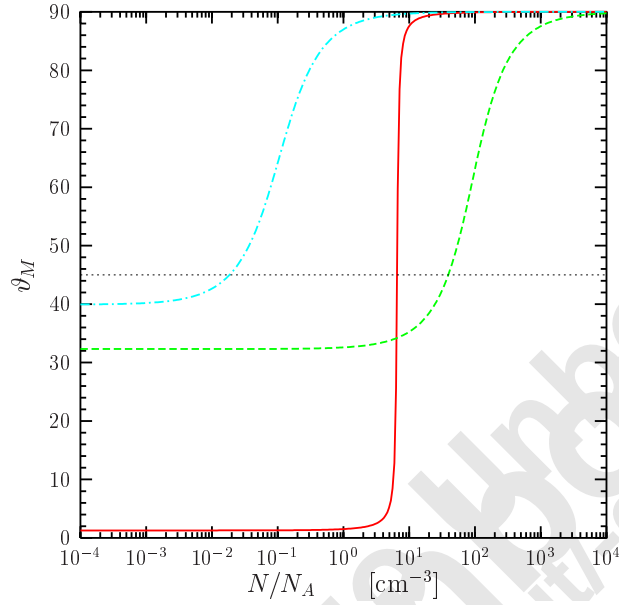


Figure 17: Effective mixing angle in matter as a function of the effective number density $N = N_e$ for $\nu_e \rightarrow \nu_{\mu,\tau}$ transitions and $N = N_e - N_n/2$ for $\nu_e \rightarrow \nu_s$ transitions. Energy: $E = 5$ MeV. Solid line: $\Delta m^2 = 5 \times 10^{-6} \text{ eV}^2$, $\tan^2 \vartheta = 5 \times 10^{-4}$ (typical SMA). Dashed line: $\Delta m^2 = 7 \times 10^{-5} \text{ eV}^2$, $\tan^2 \vartheta = 0.4$ (typical LMA). Dash-dotted line: $\Delta m^2 = 8 \times 10^{-8} \text{ eV}^2$, $\tan^2 \vartheta = 0.7$ (typical LOW).

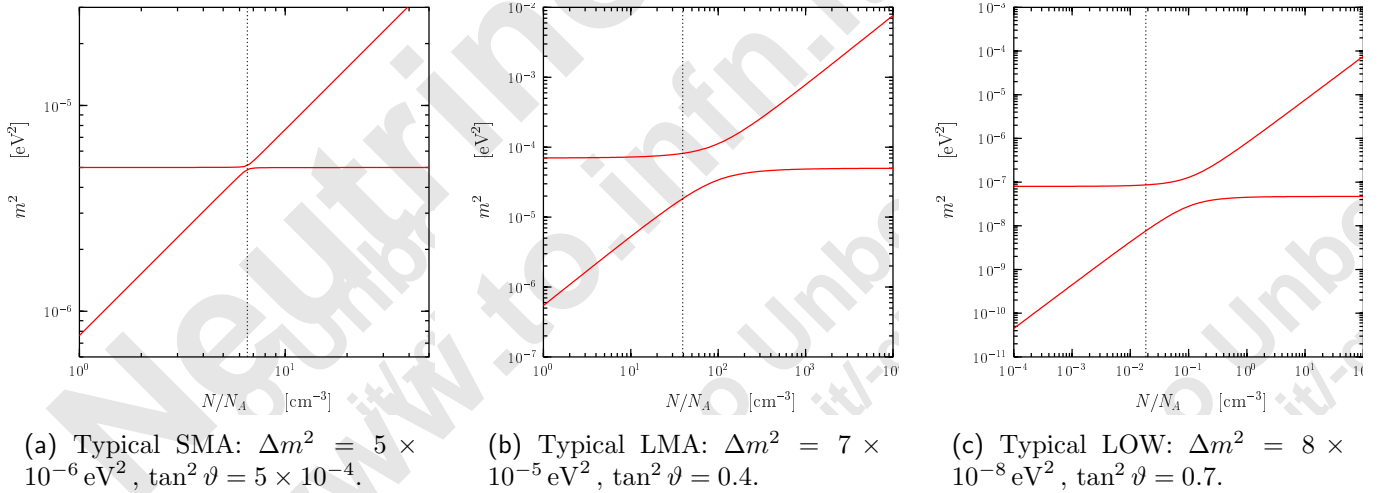
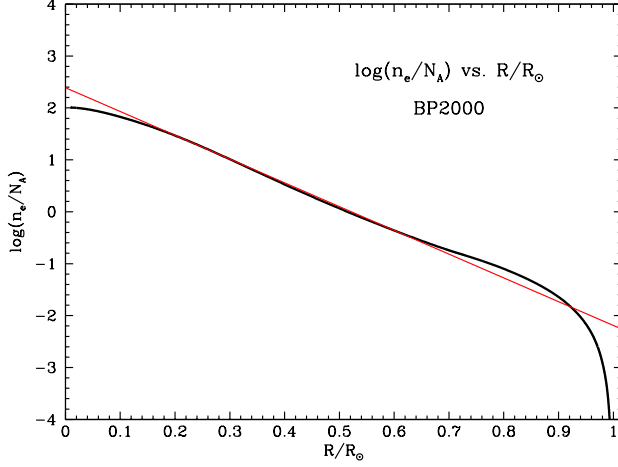


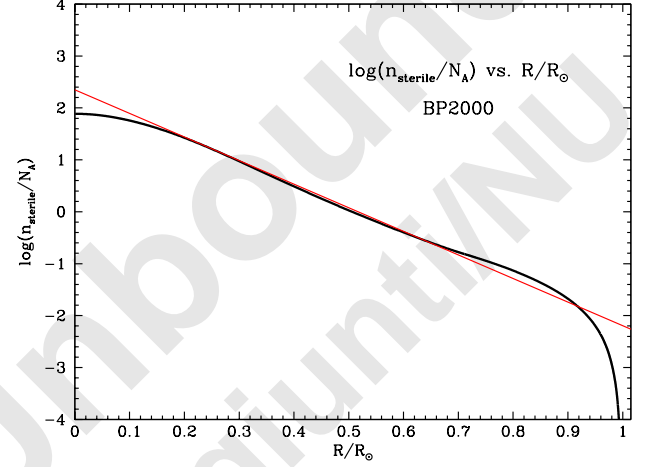
Figure 18: Effective squared masses in matter (35) as functions of the effective number density $N = N_e$ for $\nu_e \rightarrow \nu_{\mu,\tau}$ transitions and $N = N_e - N_n/2$ for $\nu_e \rightarrow \nu_s$ transitions, assuming $m_1 = 0$. Energy: $E = 5$ MeV. The dotted vertical lines show the location of the resonance (Eq. (33)), where the effective squared-mass difference Δm_M^2 in Eq. (34) is minimal (in Figs. 18(b) and 18(c) the location of the resonance appears off-center because of the logarithmic scale).

exponential approximation of electron number density in the Sun [30]:

$$N_e(R) = N_e(0) \exp\left(-\frac{R}{R_0}\right), \quad N_e(0) = 245 \text{ mol/cm}^3, \quad R_0 = \frac{R_\odot}{10.54} \quad (41)$$



(a) The electron number density, $n_e = N_e$, versus solar radius in the BP2000 SSM. The straight line represents the exponential approximation in Eq. (41).



(b) Number density of scatterers $n_{\text{sterile}} = N_e - N_n/2$ relevant for $\nu_e \rightarrow \nu_s$ transitions versus solar radius in the BP2000 SSM.

Figure 19: Figures taken from Ref. [46]. Precise numerical values are available at Ref. [28].

average ν_e survival probability after MSW transitions in Sun (Parke formula) [142]:

$$P_{\nu_e \rightarrow \nu_e}^{\text{sun}} = \frac{1}{2} + \left(\frac{1}{2} - P_c\right) \cos 2\vartheta \cos 2\vartheta_M^0, \quad \vartheta_M^0 = \text{effective mixing angle at production} \quad (42)$$

$$\nu_1 \leftrightarrow \nu_2 \text{ crossing probability [124]:} \quad P_c = \frac{\exp\left(-\frac{\pi}{2}\gamma F\right) - \exp\left(-\frac{\pi}{2}\gamma \frac{F}{\sin^2 \vartheta}\right)}{1 - \exp\left(-\frac{\pi}{2}\gamma \frac{F}{\sin^2 \vartheta}\right)} \quad (43)$$

$$\gamma = \frac{\Delta m^2 \sin^2 2\vartheta}{2E \cos 2\vartheta \left| \frac{d \ln A}{dR} \right|_{\text{res}}} \quad (44)$$

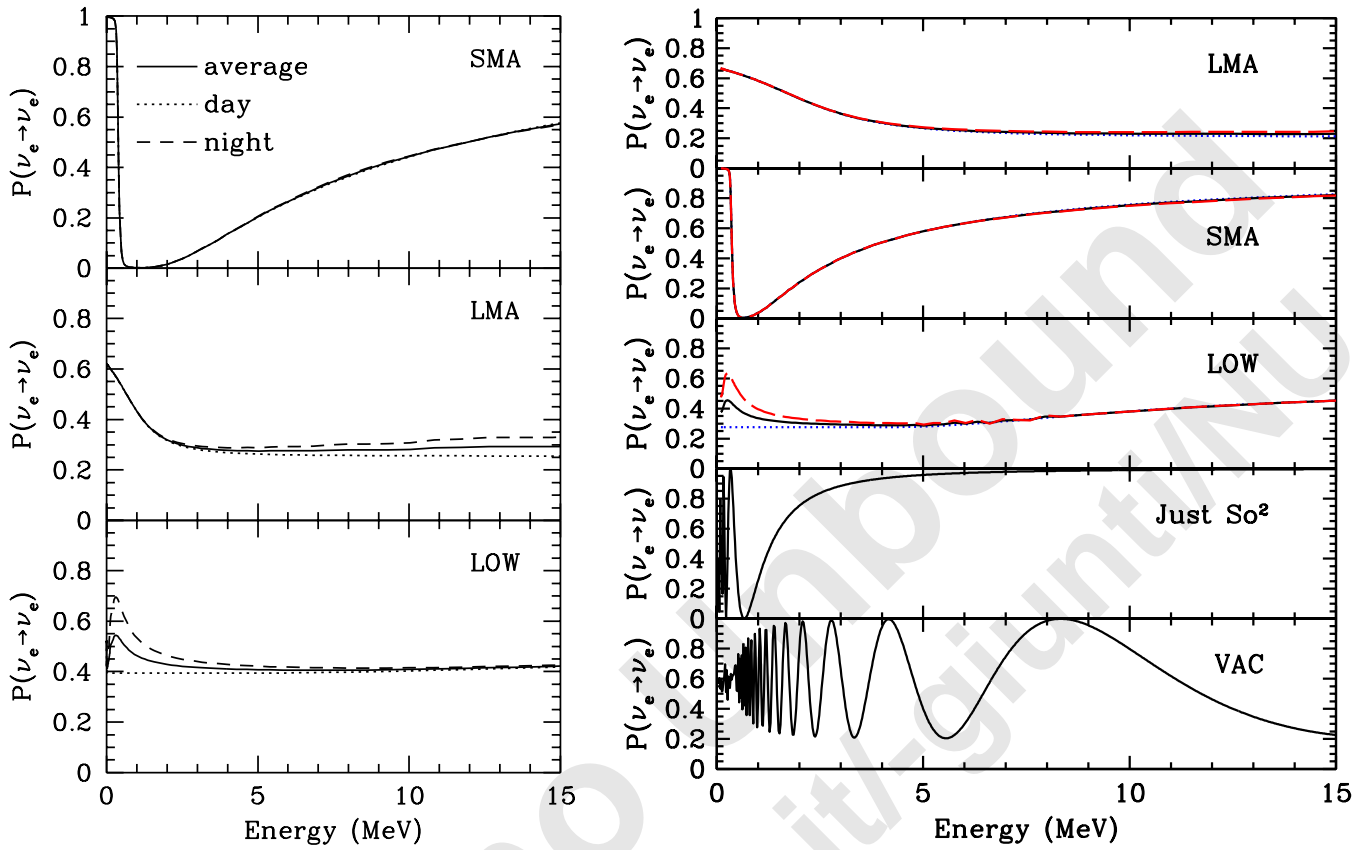
$$A \propto R \text{ [142, 109, 149, 144, 124, 48]:} \quad F = 1 \quad (45)$$

$$A \propto 1/R \text{ [124]:} \quad F = (1 - \tan^2 \vartheta)^2 / (1 + \tan^2 \vartheta) \quad (46)$$

$$A \propto \exp(-R) \text{ [149, 157, 145, 146, 48]:} \quad F = 1 - \tan^2 \vartheta \quad (47)$$

$$\text{practical prescription [127]: use Eq. (47) and} \quad \begin{cases} \text{numerical} \left| \frac{d \ln A}{dR} \right|_{\text{res}} & \text{for } R \leq 0.904R_\odot \\ \left| \frac{d \ln A}{dR} \right|_{\text{res}} \rightarrow \frac{18.9}{R_\odot} & \text{for } R > 0.904R_\odot \end{cases} \quad (48)$$

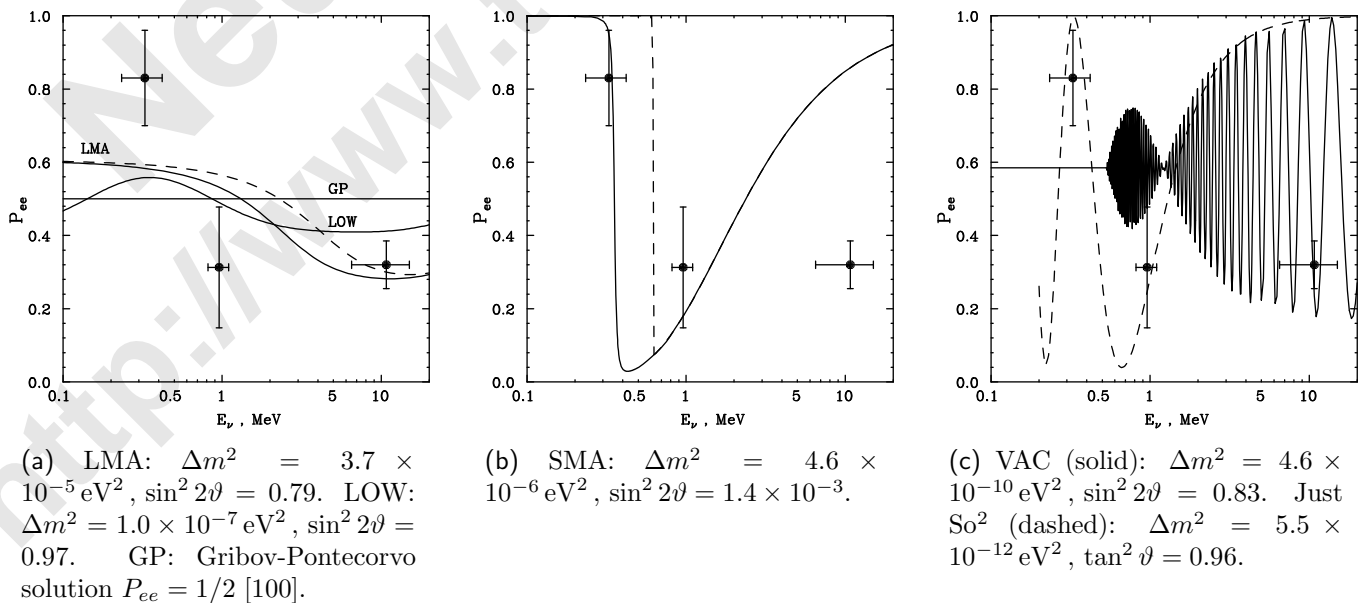
$$\nu_e \text{ regeneration in Earth [135, 50]:} \quad P_{\nu_e \rightarrow \nu_e}^{\text{sun+earth}} = P_{\nu_e \rightarrow \nu_e}^{\text{sun}} + \frac{(1 - 2P_{\nu_e \rightarrow \nu_e}^{\text{sun}})(P_{\nu_2 \rightarrow \nu_e}^{\text{earth}} - \sin^2 \vartheta)}{\cos 2\vartheta} \quad (49)$$



(a) SMA: $\Delta m^2 = 5.0 \times 10^{-6} \text{ eV}^2$, $\sin^2 2\vartheta = 3.5 \times 10^{-3}$. LMA: $\Delta m^2 = 1.6 \times 10^{-5} \text{ eV}^2$, $\sin^2 2\vartheta = 0.57$. LOW: $\Delta m^2 = 7.9 \times 10^{-8} \text{ eV}^2$, $\sin^2 2\vartheta = 0.95$. Figure from Ref. [42].

(b) LMA: $\Delta m^2 = 4.2 \times 10^{-5} \text{ eV}^2$, $\tan^2 \vartheta = 0.26$. SMA: $\Delta m^2 = 5.2 \times 10^{-6} \text{ eV}^2$, $\tan^2 \vartheta = 5.5 \times 10^{-4}$. LOW: $\Delta m^2 = 7.6 \times 10^{-8} \text{ eV}^2$, $\tan^2 \vartheta = 0.72$. Just So²: $\Delta m^2 = 5.5 \times 10^{-12} \text{ eV}^2$, $\tan^2 \vartheta = 1.0$. VAC: $\Delta m^2 = 1.4 \times 10^{-10} \text{ eV}^2$, $\tan^2 \vartheta = 0.38$. Figure from Ref. [43].

Figure 20: Solar ν_e survival probability as a function of energy. Regeneration in the Earth is included.



(a) LMA: $\Delta m^2 = 3.7 \times 10^{-5} \text{ eV}^2$, $\sin^2 2\vartheta = 0.79$. LOW: $\Delta m^2 = 1.0 \times 10^{-7} \text{ eV}^2$, $\sin^2 2\vartheta = 0.97$. GP: Gribov-Pontecorvo solution $P_{ee} = 1/2$ [100].

(b) SMA: $\Delta m^2 = 4.6 \times 10^{-6} \text{ eV}^2$, $\sin^2 2\vartheta = 1.4 \times 10^{-3}$.

(c) VAC (solid): $\Delta m^2 = 4.6 \times 10^{-10} \text{ eV}^2$, $\sin^2 2\vartheta = 0.83$. Just So² (dashed): $\Delta m^2 = 5.5 \times 10^{-12} \text{ eV}^2$, $\tan^2 \vartheta = 0.96$.

Figure 21: Survival probability of electron neutrinos as a function of energy. Data points are extracted from the gallium, chlorine and boron-neutrino signals. Figures from Ref. [60].

14 Fits of current solar neutrino data

Two-Neutrino $\nu_e \rightarrow \nu_\mu, \nu_\tau$ Oscillations: [11, 56, 53, 39, 16, 80, 93, 156, 86, 85, 130]

Two-Neutrino $\nu_e \rightarrow \nu_s$ Oscillations: [38, 130]

Three-Neutrino Mixing: [85]

Four-Neutrino Mixing: [131]

Spin-Flavor Precession: [71, 59]

Neutrino Unbound
<http://www.to.infn.it/~giunti/NU>

15 $\nu_e \rightarrow \nu_\mu, \nu_\tau$ allowed regions from Ref. [39]

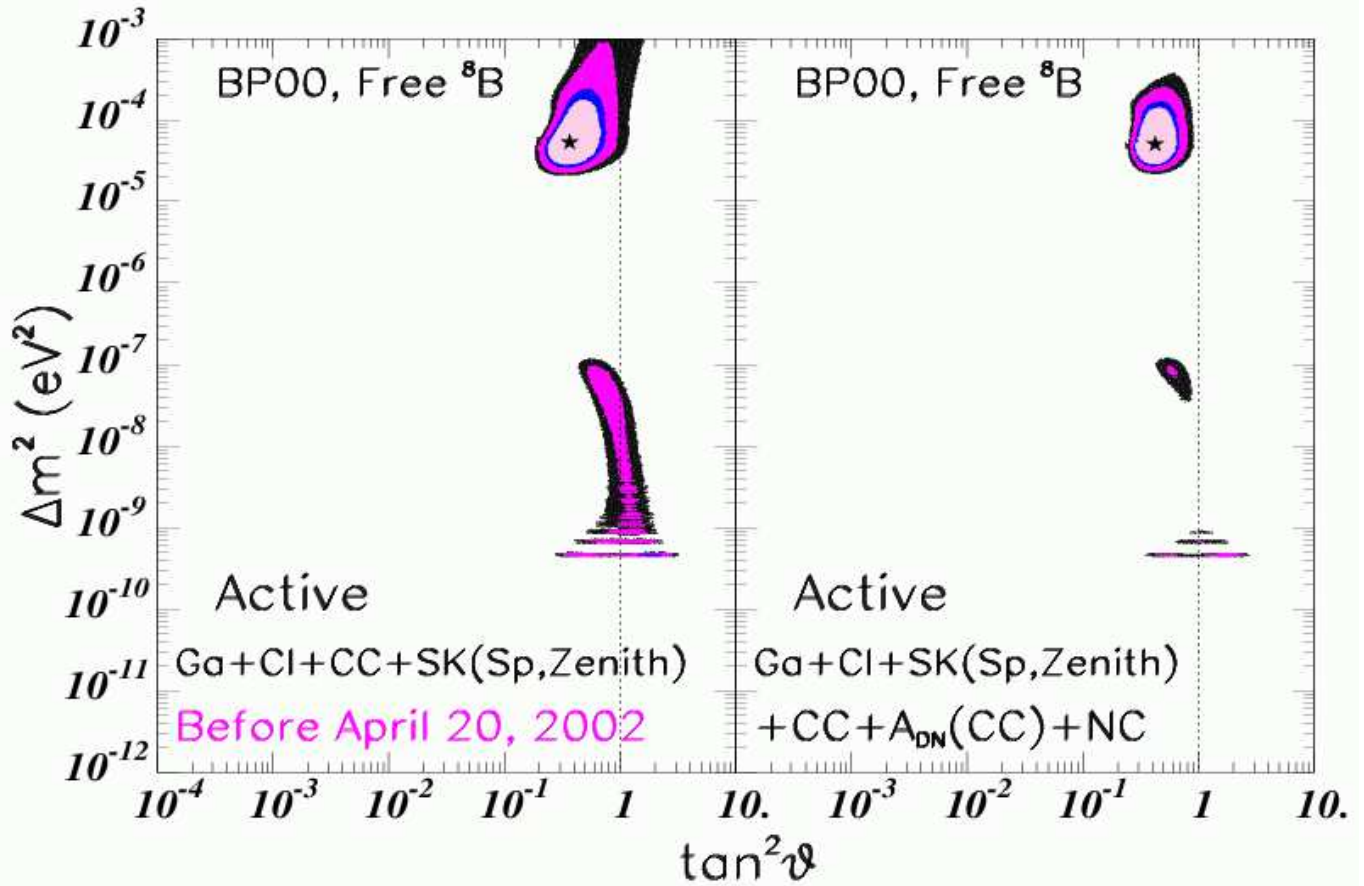


Figure 22: 90%, 95%, 99%, 99.73% (3σ) C.L. regions. The star marks the best-fit point.

$$\text{Best-fit (LMA): } \tan^2 \vartheta \simeq 0.42, \quad \Delta m^2 \simeq 5.0 \times 10^{-5} \text{ eV}^2 \quad (50)$$

99.73% C.L. (3σ) allowed intervals:

$$\begin{aligned} \text{LMA:} & \quad 0.24 < \tan^2 \vartheta < 0.89, & \quad 2.3 \times 10^{-5} < \Delta m^2/\text{eV}^2 < 3.7 \times 10^{-4} \\ \text{LOW:} & \quad 0.43 < \tan^2 \vartheta < 0.86, & \quad 3.5 \times 10^{-8} < \Delta m^2/\text{eV}^2 < 1.2 \times 10^{-7} \end{aligned} \quad (51)$$

16 $\nu_e \rightarrow \nu_{\mu}, \nu_{\tau}$ allowed regions from Ref. [86]

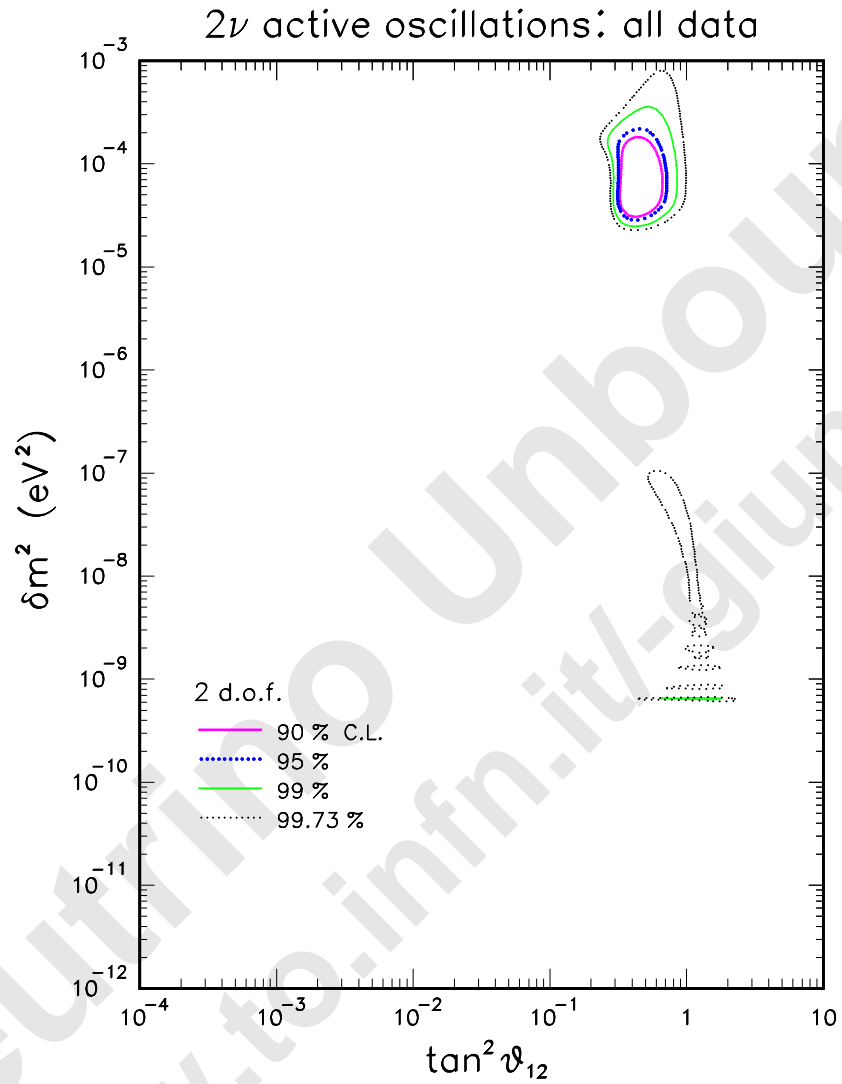


Figure 23: 90%, 95%, 99%, 99.73% (3σ) C.L. regions.

Best-fit (LMA): $\tan^2 \vartheta \simeq 0.42$, $\Delta m^2 \simeq 5.5 \times 10^{-5} \text{ eV}^2$ (52)

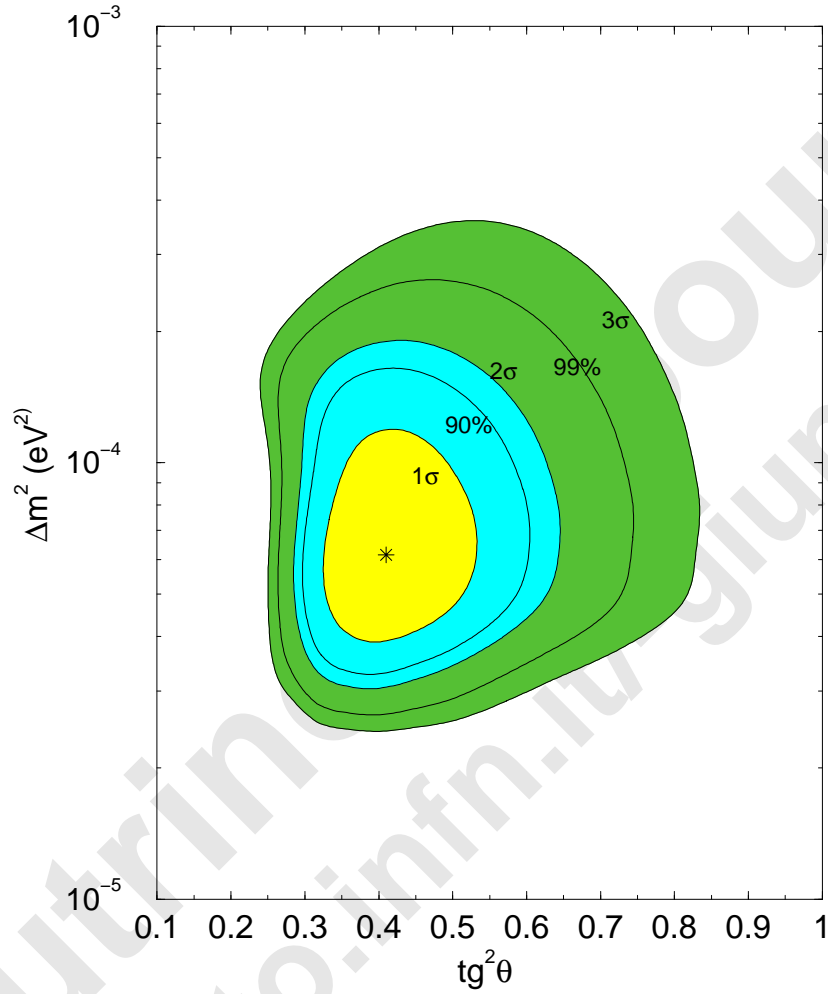
17 $\nu_e \rightarrow \nu_\mu, \nu_\tau$ allowed regions from Ref. [80]

Figure 24: 68.3% (1σ) 90%, 95.5% (2σ), 99%, 99.73% (3σ) C.L. regions. The star marks the best-fit point.

$$\text{Best-fit (LMA):} \quad \tan^2 \vartheta \simeq 0.41, \quad \Delta m^2 \simeq 6.15 \times 10^{-5} \text{ eV}^2 \quad (53)$$

99.73% C.L. (3σ) allowed intervals:

$$\text{LMA:} \quad 0.2 < \tan^2 \vartheta < 0.84, \quad 2.3 \times 10^{-5} < \Delta m^2 / \text{eV}^2 < 3.6 \times 10^{-4} \quad (54)$$

18 KamLAND \Rightarrow LMA

Kamioka Liquid scintillator Anti-Neutrino Detector, long-baseline reactor $\bar{\nu}_e$ experiment

Kamioka mine (200 km west of Tokyo), 1000 m underground, 2700 m.w.e.

average distance from reactors: 180 km
 6.7% of flux from one reactor at 88 km
 79% of flux from 26 reactors at 138–214 km
 14.3% of flux from other reactors at >295 km

1 kt liquid scintillator detector: $\bar{\nu}_e + p \rightarrow e^+ + n$, energy threshold: $E_{\text{th}}^{\bar{\nu}_e p} = 1.8$ MeV

data taking: 4 March – 6 October 2002, 145.1 days (162 ton yr) [83]

$$\text{expected number of reactor neutrino events (no osc.): } N_{\text{expected}}^{\text{KamLAND}} = 86.8 \pm 5.6 \quad (55)$$

$$\text{expected number of background events: } N_{\text{background}}^{\text{KamLAND}} = 0.95 \pm 0.99 \quad (56)$$

$$\text{observed number of neutrino events: } N_{\text{observed}}^{\text{KamLAND}} = 54 \quad (57)$$

$$\frac{N_{\text{observed}}^{\text{KamLAND}} - N_{\text{background}}^{\text{KamLAND}}}{N_{\text{expected}}^{\text{KamLAND}}} = 0.611 \pm 0.085 \pm 0.041 \quad [83] \quad (58)$$

99.95% C.L. evidence of $\bar{\nu}_e$ disappearance

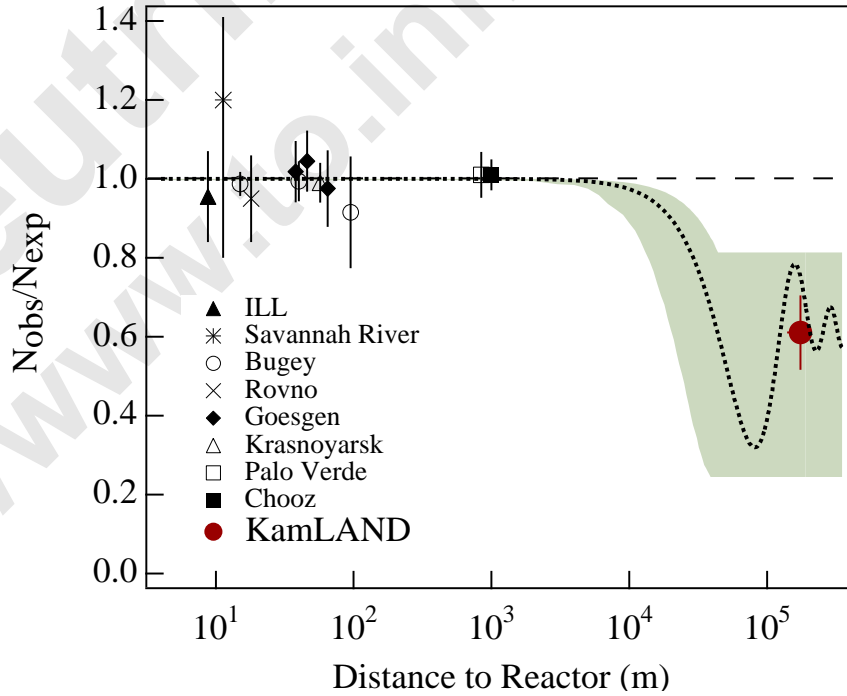
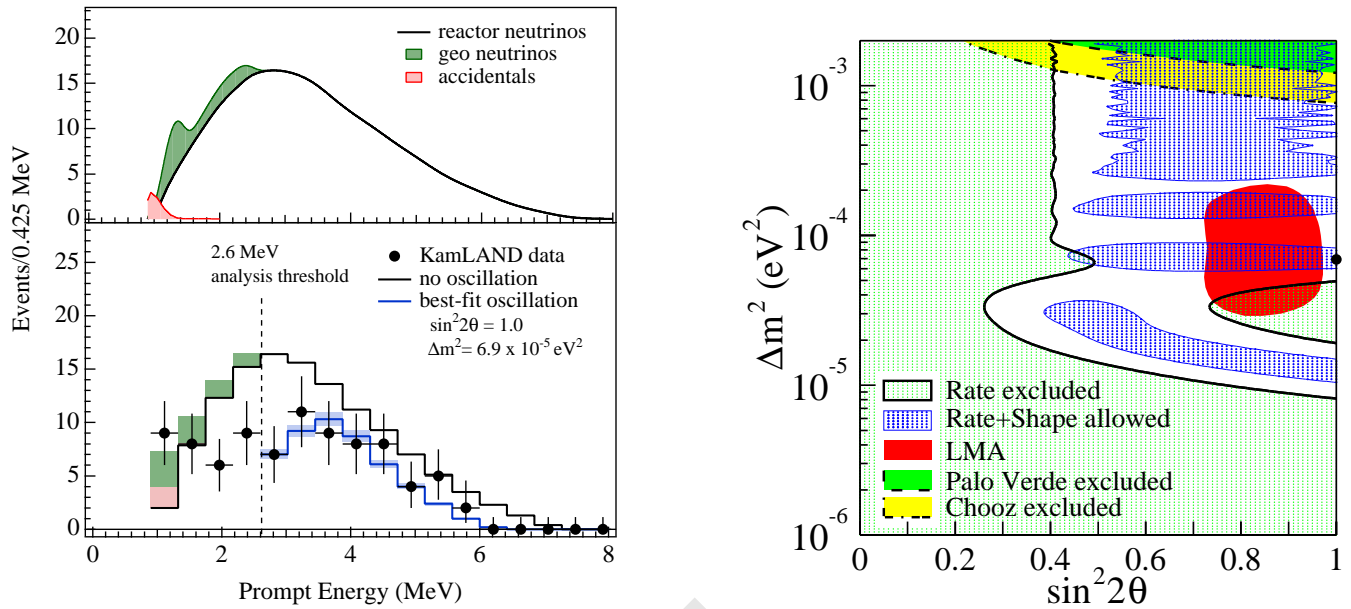


Figure 25: The ratio of measured to expected $\bar{\nu}_e$ flux from reactor experiments. The shaded region indicates the range of flux predictions corresponding to the 95% C.L. LMA region found in a global analysis of the solar neutrino data [86]. The dotted curve corresponds to the best-fit values $\Delta m_{\text{sol}}^2 = 5.5 \times 10^{-5} \text{ eV}^2$ and $\sin^2 2\theta_{\text{sol}} = 0.83$ found in Ref. [86]. Figure from Ref. [83].



(a) Upper panel: Expected reactor $\bar{\nu}_e$ energy spectrum with contributions of $\bar{\nu}_{\text{geo}}$ (antineutrinos emitted by ^{238}U and ^{232}Th decays in the earth) and accidental background. Lower panel: Energy spectrum of the observed prompt events (solid circles with error bars), along with the expected no oscillation spectrum (upper histogram, with $\bar{\nu}_{\text{geo}}$ and accidentals shown) and best fit (lower histogram) including neutrino oscillations. The shaded band indicates the systematic error in the best-fit spectrum. The vertical dashed line corresponds to the analysis threshold at 2.6 MeV.

(b) KamLAND excluded regions of neutrino oscillation parameters $\Delta m_{\text{KamLAND}}^2 = \Delta m^2$ and $\sin^2 2\vartheta_{\text{KamLAND}} = \sin^2 2\theta$ for the rate analysis and allowed regions for the combined rate and energy spectrum analysis at 95% C.L. At the top are the 95% C.L. excluded region from CHOOZ [26, 27] and Palo Verde [67] experiments, respectively. The dark area is the 95% C.L. LMA allowed region obtained in Ref. [86]. The thick dot indicates the best fit of the KamLAND data in Eq. (60).

Figure 26: Figures taken from Ref. [83].

$$E_{\text{prompt}} = E_{\bar{\nu}_e} + m_p - m_n - \bar{T}_n + m_e = E_{\bar{\nu}_e} - \bar{T}_n - 0.8 \text{ MeV} \quad (59)$$

\bar{T}_n = average kinetic energy of the neutron; m_e comes from annihilation of final e^+ with e^- in medium

$$\text{best fit: } \Delta m_{\text{KamLAND}}^2 = 6.9 \times 10^{-5} \text{ eV}^2, \quad \sin^2 2\vartheta_{\text{KamLAND}} = 1 \quad [83] \quad (60)$$

19 Fits of reactor + solar neutrino data

[55, 88, 132, 54, 40, 115, 17, 79, 49]

20 Allowed reactor + solar region from Ref. [88]

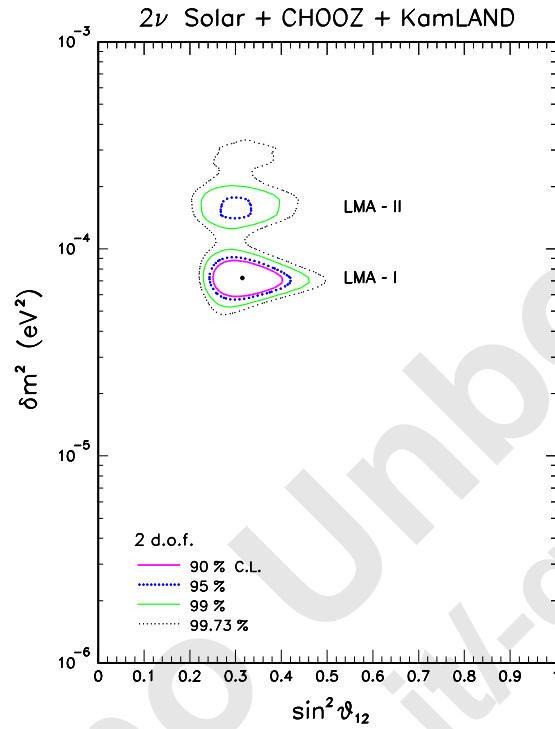


Figure 27: Allowed 90%, 95%, 99%, 99.73% (3σ) C.L. regions. The black dot is the best-fit point.

$$\text{Best-fit: } \sin^2 \vartheta \simeq 0.315, \quad \Delta m^2 \simeq 7.3 \times 10^{-5} \text{ eV}^2 \quad (61)$$

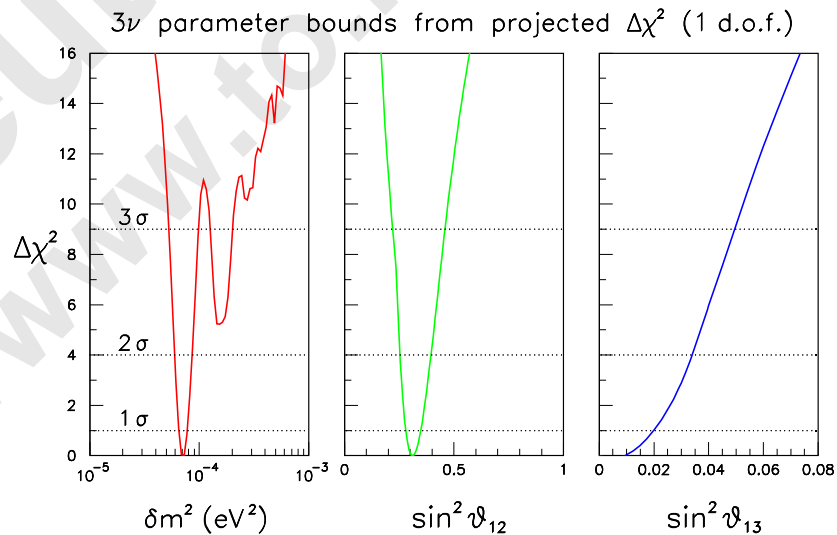


Figure 28: Three-neutrino oscillations: projections of the global $\Delta\chi^2$ function on the $\delta m^2 = \Delta m_{\text{sol}}^2$, $\sin^2 \vartheta_{12}$, $\sin^2 \vartheta_{13}$ axes. The $n\sigma$ bounds on each parameter correspond to $\Delta\chi^2 = n^2$.

21 Allowed reactor + solar region from Ref. [132]

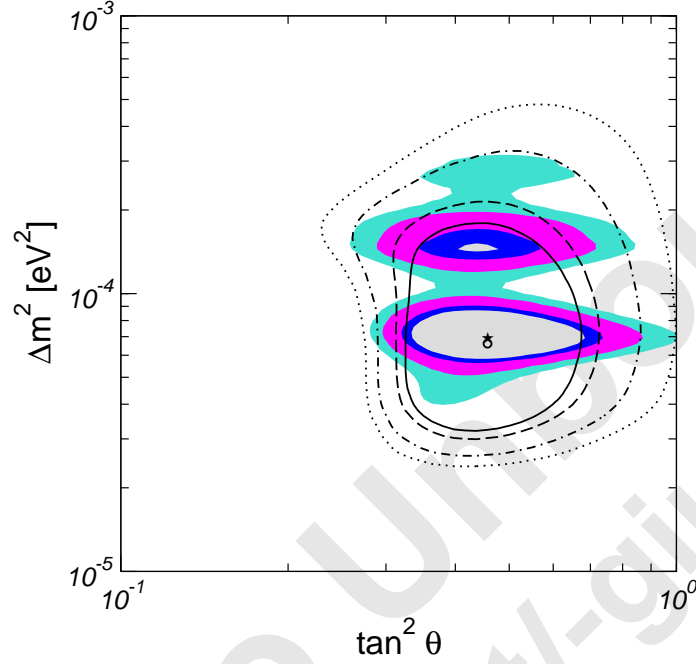


Figure 29: Allowed 90%, 95%, 99%, 99.73% (3σ) C.L. regions. The hollow lines are the allowed regions from solar and CHOOZ data alone. The star (dot) is the best-fit point from the combined (solar and CHOOZ only) analysis.

$$\text{Best-fit: } \tan^2 \vartheta \simeq 0.46, \quad \Delta m^2 \simeq 6.9 \times 10^{-5} \text{ eV}^2 \quad (62)$$

$$99.73\% \text{ C.L. } (3\sigma) \text{ allowed interval: } 0.29 < \tan^2 \vartheta < 0.86 \quad (63)$$

$$99.73\% \text{ C.L. } (3\sigma) \text{ allowed intervals: } \begin{cases} 5.1 \times 10^{-5} < \Delta m^2/\text{eV}^2 < 9.7 \times 10^{-5} \\ 1.2 \times 10^{-4} < \Delta m^2/\text{eV}^2 < 1.9 \times 10^{-4} \end{cases} \quad (64)$$

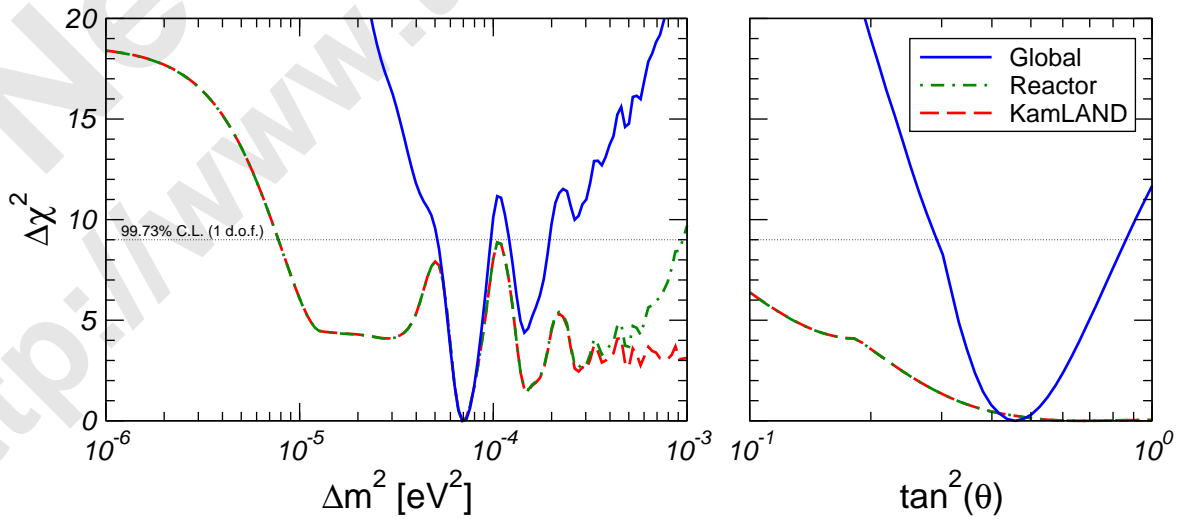


Figure 30: $\Delta\chi^2$ versus Δm^2 and $\tan^2 \vartheta$. The dashed line refers to KamLAND alone. The dot-dashed line corresponds to the full reactor data sample, including both KamLAND and Chooz. The solid line refers to the global analysis of the complete solar and reactor data.

22 Allowed reactor + solar region from Ref. [40]

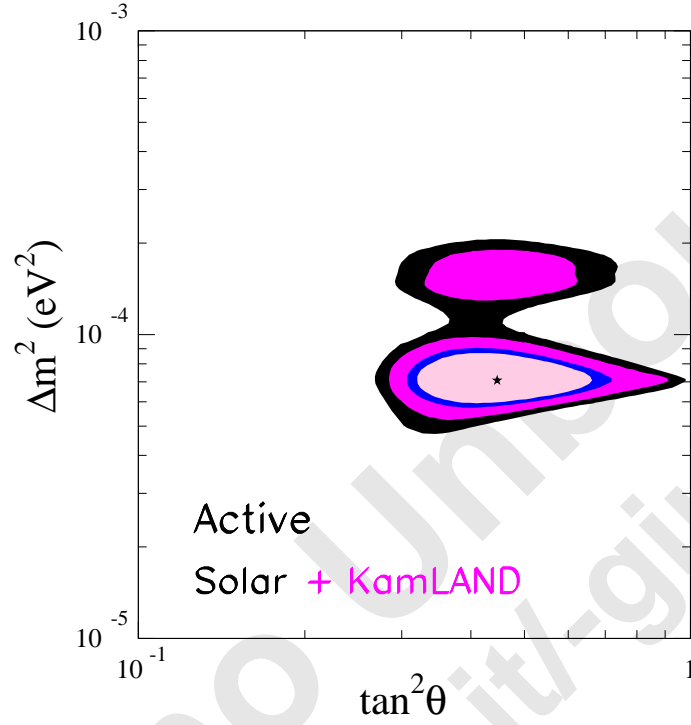


Figure 31: Allowed 90%, 95%, 99%, 99.73% (3σ) C.L. regions. The global best-fit point is marked by a star.

$$\text{Best-fit: } \tan^2 \vartheta \simeq 0.45, \quad \Delta m^2 \simeq 7.1 \times 10^{-5} \text{ eV}^2, \quad \frac{\Phi_{sB}}{\Phi_{sB}^{\text{SSM}}} = 1.00 \quad (65)$$

$$99.73\% \text{ C.L. } (3\sigma) \text{ allowed interval: } 0.28 < \tan^2 \vartheta < 0.91 \quad (66)$$

$${}^8\text{B neutrino flux: } \Phi_{sB} = 1.00 \pm 0.06 \Phi_{sB}^{\text{SSM}} \quad (67)$$

$$\text{sterile neutrino component } (\nu_e \rightarrow \cos \eta \nu_a + \sin \eta \nu_s): \quad \sin^2 \eta < 0.52 (3\sigma) \quad (68)$$

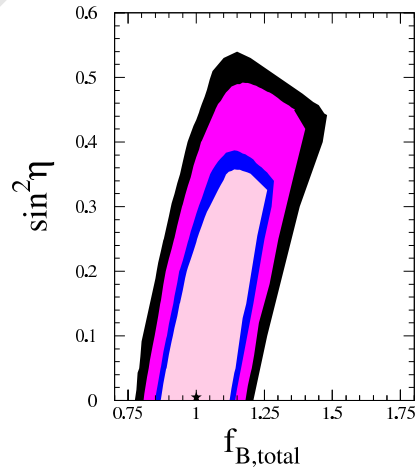


Figure 32: Allowed 90%, 95%, 99%, 99.73% (3σ) C.L. regions in the $f_{B,\text{total}} - \sin^2 \eta$ plane, with $f_{B,\text{total}} = \Phi_{sB}/\Phi_{sB}^{\text{SSM}}$. The best-fit point is marked by a star.

23 Allowed reactor + solar region from Ref. [79]

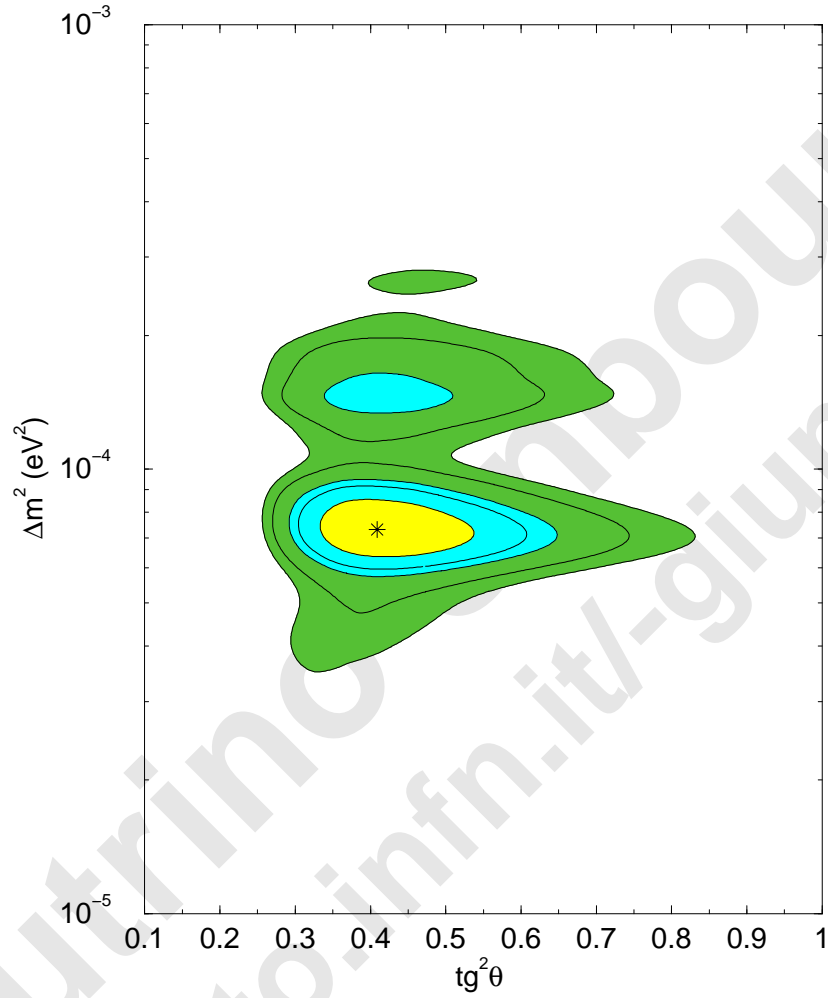


Figure 33: Allowed 68.3% (1σ) 90%, 95%, 99%, 99.73% (3σ) C.L. regions. The best-fit point is marked by a star.

$$\text{Best-fit: } \tan^2 \vartheta \simeq 0.41, \quad \Delta m^2 \simeq 7.3 \times 10^{-5} \text{ eV}^2, \quad \frac{\Phi_{sB}}{\Phi_{sB}^{SSM}} = 1.05 \quad (69)$$

$$99.73\% \text{ C.L. } (3\sigma) \text{ bounds: } \Delta m^2 < 2.8 \times 10^{-4} \text{ eV}^2, \quad \tan^2 \vartheta < 0.84 \quad (70)$$

Bibliography

- [1] A. I. Abazov et al., "Search for neutrinos from sun using the reaction ${}^{71}\text{Ga}(\nu_e, e^-){}^{71}\text{Ge}$ ", *Phys. Rev. Lett.*, 67, 3332–3335, 1991.
- [2] D. N. Abdurashitov et al., "Results from SAGE", *Phys. Lett.*, B328, 234–248, 1994.
- [3] D. N. Abdurashitov et al., "The Russian-American gallium experiment (SAGE) Cr neutrino source measurement", *Phys. Rev. Lett.*, 77, 4708–4711, 1996.
- [4] J. N. Abdurashitov et al., "Measurement of the response of the Russian-American gallium experiment to neutrinos from a Cr-51 source", *Phys. Rev.*, C59, 2246–2263, 1999, hep-ph/9803418.
- [5] J. N. Abdurashitov et al., "Measurement of the solar neutrino capture rate by SAGE and implications for neutrino oscillations in vacuum", *Phys. Rev. Lett.*, 83, 4686–4689, 1999, astro-ph/9907131.
- [6] J. N. Abdurashitov et al., "Measurement of the solar neutrino capture rate with gallium metal", *Phys. Rev.*, C60, 055801, 1999, astro-ph/9907113.
- [7] J. N. Abdurashitov et al., "Measurement of the Solar Neutrino Capture Rate by the Russian-American Gallium Solar Neutrino Experiment During One Half of the 22-Year Cycle of Solar Activity", *J. Exp. Theor. Phys.*, 95, 181–193, 2002, astro-ph/0204245.
- [8] A. Acker, S. Pakvasa, and J. Pantaleone, "The Solar neutrino problem: Some old solutions revisited", *Phys. Rev.*, D43, 1754–1758, 1991.
- [9] Q. R. Ahmad et al., "Measurement of the charged current interactions produced by B-8 solar neutrinos at the Sudbury Neutrino Observatory", *Phys. Rev. Lett.*, 87, 071301, 2001, nucl-ex/0106015.
- [10] Q. R. Ahmad et al., "Direct Evidence for Neutrino Flavor Transformation from Neutral-Current Interactions in the Sudbury Neutrino Observatory", *Phys. Rev. Lett.*, 89, 011301, 2002, nucl-ex/0204008.
- [11] Q. R. Ahmad et al., "Measurement of Day and Night Neutrino Energy Spectra at SNO and Constraints on Neutrino Mixing Parameters", *Phys. Rev. Lett.*, 89, 011302, 2002, nucl-ex/0204009.
- [12] E. K. Akhmedov, "Parametric resonance of neutrino oscillations and passage of solar and atmospheric neutrinos through the earth", *Nucl. Phys.*, B538, 25–51, 1999, hep-ph/9805272.
- [13] E. K. Akhmedov, "Resonance enhancement of the neutrino spin precession in matter and the solar neutrino problem", *Sov. J. Nucl. Phys.*, 48, 382–383, 1988.
- [14] E. K. Akhmedov, "Resonant amplification of neutrino spin rotation in matter and the solar-neutrino problem", *Phys. Lett.*, B213, 64, 1988.
- [15] E. K. Akhmedov, "Mutual influence of resonant spin flavor precession and resonant neutrino oscillations", *Sov. Phys. JETP*, 68, 690–696, 1989.
- [16] P. Aliani, V. Antonelli, R. Ferrari, M. Picariello, and E. Torrente-Lujan, "Determination of neutrino mixing parameters after SNO oscillation evidence", 2002, hep-ph/0205053.
- [17] P. Aliani, V. Antonelli, M. Picariello, and E. Torrente-Lujan, "Neutrino mass parameters from Kamland, SNO and other solar evidence", 2002, hep-ph/0212212.

- [18] M. Altmann et al., “GNO solar neutrino observations: Results for GNO I”, *Phys. Lett.*, B490, 16–26, 2000, hep-ex/0006034.
- [19] L. W. Alvarez, 1949, University of California Radiation Laboratory Report UCRL 328.
- [20] S. Ando, Y. H. Song, T. S. Park, H. W. Fearing, and K. Kubodera, “Solar-neutrino reactions on deuteron in effective field theory”, 2002, nucl-th/0206001.
- [21] P. Anselmann et al., “Solar neutrinos observed by GALLEX at Gran Sasso.”, *Phys. Lett.*, B285, 376–389, 1992.
- [22] P. Anselmann et al., “GALLEX solar neutrino observations: The Results from GALLEX-I and early results from GALLEX-II”, *Phys. Lett.*, B314, 445–458, 1993.
- [23] P. Anselmann et al., “GALLEX results from the first 30 solar neutrino runs”, *Phys. Lett.*, B327, 377–385, 1994.
- [24] P. Anselmann et al., “First results from the Cr-51 neutrino source experiment with the GALLEX detector”, *Phys. Lett.*, B342, 440–450, 1995.
- [25] P. Anselmann et al., “GALLEX solar neutrino observations: Complete results for GALLEX II”, *Phys. Lett.*, B357, 237–247, 1995.
- [26] M. Apollonio et al., “Limits on neutrino oscillations from the CHOOZ experiment”, *Phys. Lett.*, B466, 415–430, 1999, hep-ex/9907037.
- [27] M. Apollonio et al., “Search for neutrino oscillations on a long base-line at the CHOOZ nuclear power station”, 2003, hep-ex/0301017.
- [28] J. N. Bahcall, <http://www.sns.ias.edu/~jnb>.
- [29] J. N. Bahcall, “Solar neutrinos. I: Theoretical”, *Phys. Rev. Lett.*, 12, 300–302, 1964.
- [30] J. N. Bahcall, *Neutrino Astrophysics*, Cambridge University Press, 1989.
- [31] J. N. Bahcall, “The Be-7 solar neutrino line: A Reflection of the central temperature distribution of the sun”, *Phys. Rev.*, D49, 3923–3945, 1994.
- [32] J. N. Bahcall, “Gallium solar neutrino experiments: Absorption cross sections, neutrino spectra, and predicted event rates”, *Phys. Rev.*, C56, 3391, 1997, hep-ph/9710491.
- [33] J. N. Bahcall, “The luminosity constraint on solar neutrino fluxes”, *Phys. Rev.*, C65, 025801, 2002, hep-ph/0108148.
- [34] J. N. Bahcall, S. Basu, and M. H. Pinsonneault, “How uncertain are solar neutrino predictions?”, *Phys. Lett.*, B433, 1–8, 1998, astro-ph/9805135.
- [35] J. N. Bahcall and J. Davis, Raymond, “The evolution of neutrino astronomy”, *Publ. Astron. Soc. Pac.*, 112, 429–433, 2000, astro-ph/9911486.
- [36] J. N. Bahcall and R. Davis, “The beginning of a new science”, *CERN Cour.*, 40N6, 17–21, 2000, <http://www.cerncourier.com/main/article/40/6/18>.
- [37] J. N. Bahcall et al., “Standard Neutrino Spectrum from ${}^8\text{B}$ Decay”, *Phys. Rev.*, C54, 411–422, 1996, nucl-th/9601044.

- [38] J. N. Bahcall, M. C. Gonzalez-Garcia, and C. Pena-Garay, "If sterile neutrinos exist, how can one determine the total B-8 and Be-7 solar neutrino fluxes?", *Phys. Rev.*, C66, 035802, 2002, hep-ph/0204194.
- [39] J. N. Bahcall, M. C. Gonzalez-Garcia, and C. Pena-Garay, "Before and after: How has the SNO neutral current measurement changed things?", *JHEP*, 07, 054, 2002, hep-ph/0204314.
- [40] J. N. Bahcall, M. C. Gonzalez-Garcia, and C. Pena-Garay, "Solar Neutrinos Before and After KamLAND", 2002, hep-ph/0212147.
- [41] J. N. Bahcall, W. F. Huebner, S. H. Lubow, P. D. Parker, and R. K. Ulrich, "Standard solar models and the uncertainties in predicted capture rates of solar neutrinos", *Rev. Mod. Phys.*, 54, 767, 1982.
- [42] J. N. Bahcall, P. I. Krastev, and A. Y. Smirnov, "Where do we stand with solar neutrino oscillations?", *Phys. Rev.*, D58, 096016, 1998, hep-ph/9807216.
- [43] J. N. Bahcall, P. I. Krastev, and A. Y. Smirnov, "Solar neutrinos: Global analysis and implications for SNO", *JHEP*, 05, 015, 2001, hep-ph/0103179.
- [44] J. N. Bahcall and M. H. Pinsonneault, "Standard solar models, with and without helium diffusion and the solar neutrino problem", *Rev. Mod. Phys.*, 64, 885–926, 1992.
- [45] J. N. Bahcall and M. H. Pinsonneault, "Solar models with helium and heavy element diffusion", *Rev. Mod. Phys.*, 67, 781–808, 1995, hep-ph/9505425.
- [46] J. N. Bahcall, M. H. Pinsonneault, and S. Basu, "Solar models: Current epoch and time dependences, neutrinos, and helioseismological properties", *Astrophys. J.*, 555, 990–1012, 2001, astro-ph/0010346.
- [47] J. N. Bahcall and R. K. Ulrich, "Solar models, neutrino experiments and helioseismology", *Rev. Mod. Phys.*, 60, 297–372, 1988.
- [48] A. B. Balantekin, "Exact solutions for matter-enhanced neutrino oscillations", *Phys. Rev.*, D58, 013001, 1998, hep-ph/9712304.
- [49] A. Balantekin and H. Yuksel, "Global Analysis of Solar Neutrino and KamLAND Data", 2002, hep-ph/0301072.
- [50] A. J. Baltz and J. Weneser, "Effect of transmission through the earth on neutrino oscillations", *Phys. Rev.*, D35, 528, 1987.
- [51] A. J. Baltz and J. Weneser, "Matter oscillations: neutrino transformation in the sun and regeneration in the earth", *Phys. Rev.*, D37, 3364, 1988.
- [52] A. J. Baltz and J. Weneser, "Implication of gallium results on the possibility of observing day - night matter oscillations at SNO, Super- Kamiokande and Borexino", *Phys. Rev.*, D50, 5971–5979, 1994.
- [53] A. Bandyopadhyay, S. Choubey, S. Goswami, and D. P. Roy, "Implications of the first neutral current data from SNO for solar neutrino oscillation", *Phys. Lett.*, B540, 14–19, 2002, hep-ph/0204286.
- [54] A. Bandyopadhyay et al., "The Solar Neutrino Problem after the first results from Kamland", 2002, hep-ph/0212146.

- [55] V. Barger and D. Marfatia, “KamLAND and solar neutrino data eliminate the LOW solution”, 2002, hep-ph/0212126.
- [56] V. Barger, D. Marfatia, K. Whisnant, and B. P. Wood, “Imprint of SNO neutral current data on the solar neutrino problem”, *Phys. Lett.*, B537, 179–186, 2002, hep-ph/0204253.
- [57] V. Barger, K. Whisnant, and R. J. N. Phillips, “Realistic calculations of solar neutrino oscillations”, *Phys. Rev.*, D24, 538, 1981.
- [58] V. D. Barger, K. Whisnant, S. Pakvasa, and R. J. N. Phillips, “Matter effects on three-neutrino oscillations”, *Phys. Rev.*, D22, 2718, 1980.
- [59] J. Barranco, O. G. Miranda, T. I. Rashba, V. B. Semikoz, and J. W. F. Valle, “Confronting Spin Flavor Solutions of the Solar Neutrino Problem with current and future solar neutrino data”, *Phys. Rev.*, D66, 093009, 2002, hep-ph/0207326.
- [60] V. Berezinsky and M. Lissia, “Electron neutrino survival probability from solar-neutrino data”, *Phys. Lett.*, B521, 287–290, 2001, hep-ph/0108108.
- [61] H. A. Bethe, “Possible explanation of the solar-neutrino puzzle”, *Phys. Rev. Lett.*, 56, 1305, 1986.
- [62] S. M. Bilenky, “Neutrinos”, 2001, physics/0103091.
- [63] S. M. Bilenky and C. Giunti, “Lepton numbers in the framework of neutrino mixing”, *Int. J. Mod. Phys.*, A16, 3931–3949, 2001, hep-ph/0102320.
- [64] S. M. Bilenky, C. Giunti, and W. Grimus, “Phenomenology of neutrino oscillations”, *Prog. Part. Nucl. Phys.*, 43, 1, 1999, hep-ph/9812360.
- [65] S. M. Bilenky and S. T. Petcov, “Massive neutrinos and neutrino oscillations”, *Rev. Mod. Phys.*, 59, 671, 1987.
- [66] S. M. Bilenky and B. Pontecorvo, “Lepton mixing and neutrino oscillations”, *Phys. Rept.*, 41, 225, 1978.
- [67] F. Boehm et al., “Final results from the Palo Verde neutrino oscillation experiment”, *Phys. Rev.*, D64, 112001, 2001, hep-ex/0107009.
- [68] F. Boehm and P. Vogel, *Physics of massive neutrinos*, Cambridge University Press, 1992.
- [69] M. Butler, J.-W. Chen, and X. Kong, “Neutrino deuteron scattering in effective field theory at next-to-next-to-leading order”, *Phys. Rev.*, C63, 035501, 2001, nucl-th/0008032.
- [70] V. Castellani, S. Degl’Innocenti, G. Fiorentini, M. Lissia, and B. Ricci, “Solar neutrinos: Beyond standard solar models”, *Phys. Rept.*, 281, 309–398, 1997, astro-ph/9606180.
- [71] B. C. Chauhan and J. Pulido, “Resonance Spin Flavour Precession of Solar Neutrinos After SNO NC Data”, *Phys. Rev.*, D66, 053006, 2002, hep-ph/0206193.
- [72] M. V. Chizhov and S. T. Petcov, “New conditions for a total neutrino conversion in a medium”, *Phys. Rev. Lett.*, 83, 1096–1099, 1999, hep-ph/9903399.
- [73] M. V. Chizhov and S. T. Petcov, “Enhancing mechanisms of neutrino transitions in a medium of non-periodic constant-density layers and in the earth”, *Phys. Rev.*, D63, 073003, 2001, hep-ph/9903424.

- [74] A. Cisneros, "Effect of neutrino magnetic moment on solar neutrino observations", *Astrophys. Space Sci.*, 10, 87–92, 1971.
- [75] B. T. Cleveland et al., "Measurement of the solar electron neutrino flux with the Homestake chlorine detector", *Astrophys. J.*, 496, 505, 1998.
- [76] M. Cribier, W. Hampel, J. Rich, and D. Vignaud, "MSW regeneration of solar electron-neutrino in the earth", *Phys. Lett.*, B182, 89, 1986.
- [77] R. Davis, "Solar neutrinos. II: Experimental", *Phys. Rev. Lett.*, 12, 303–305, 1964.
- [78] A. de Gouvea, A. Friedland, and H. Murayama, "The dark side of the solar neutrino parameter space", *Phys. Lett.*, B490, 125–130, 2000, hep-ph/0002064.
- [79] P. C. de Holanda and A. Y. Smirnov, "LMA MSW solution of the solar neutrino problem and first KamLAND results", 2002, hep-ph/0212270.
- [80] P. C. de Holanda and A. Y. Smirnov, "Solar neutrinos: Global analysis with day and night spectra from SNO", 2002, hep-ph/0205241.
- [81] A. S. Dighe, Q. Y. Liu, and A. Y. Smirnov, "Coherence and the day-night asymmetry in the solar neutrino flux", 1999, hep-ph/9903329.
- [82] D. Dooling, C. Giunti, K. Kang, and C. W. Kim, "Matter effects in four-neutrino mixing", *Phys. Rev.*, D61, 073011, 2000, hep-ph/9908513.
- [83] K. Eguchi et al., "First Results from KamLAND: Evidence for Reactor Anti-Neutrino Disappearance", 2002, hep-ex/0212021.
- [84] P. Fisher, B. Kayser, and K. S. McFarland, "Neutrino mass and oscillation", *Ann. Rev. Nucl. Part. Sci.*, 49, 481, 1999, hep-ph/9906244.
- [85] G. L. Fogli et al., "Three-flavor solar neutrino oscillations with terrestrial neutrino constraints", *Phys. Rev.*, D66, 093008, 2002, hep-ph/0208026.
- [86] G. L. Fogli, E. Lisi, A. Marrone, D. Montanino, and A. Palazzo, "Getting the most from the statistical analysis of solar neutrino oscillations", *Phys. Rev.*, D66, 053010, 2002, hep-ph/0206162.
- [87] G. L. Fogli, E. Lisi, D. Montanino, and A. Palazzo, "Quasi-vacuum solar neutrino oscillations", *Phys. Rev.*, D62, 113004, 2000, hep-ph/0005261.
- [88] G. Fogli et al., "Solar neutrino oscillation parameters after first KamLAND results", 2002, hep-ph/0212127.
- [89] A. Friedland, "MSW effects in vacuum oscillations", *Phys. Rev. Lett.*, 85, 936–939, 2000, hep-ph/0002063.
- [90] A. Friedland, "On the evolution of the neutrino state inside the sun", *Phys. Rev.*, D64, 013008, 2001, hep-ph/0010231.
- [91] S. Fukuda et al., "Constraints on neutrino oscillations using 1258 days of Super-Kamiokande solar neutrino data", *Phys. Rev. Lett.*, 86, 5656–5660, 2001, hep-ex/0103033.

- [92] S. Fukuda et al., “Solar B-8 and hep neutrino measurements from 1258 days of Super-Kamiokande data”, *Phys. Rev. Lett.*, 86, 5651–5655, 2001, hep-ex/0103032.
- [93] S. Fukuda et al., “Determination of solar neutrino oscillation parameters using 1496 days of Super-Kamiokande-I data”, *Phys. Lett.*, B539, 179–187, 2002, hep-ex/0205075.
- [94] Y. Fukuda et al., “Solar neutrino data covering solar cycle 22”, *Phys. Rev. Lett.*, 77, 1683–1686, 1996.
- [95] Y. Fukuda et al., “Measurements of the solar neutrino flux from Super-Kamiokande’s first 300 days”, *Phys. Rev. Lett.*, 81, 1158–1162, 1998, hep-ex/9805021.
- [96] Y. Fukuda et al., “Constraints on neutrino oscillation parameters from the measurement of day-night solar neutrino fluxes at Super-Kamiokande”, *Phys. Rev. Lett.*, 82, 1810–1814, 1999, hep-ex/9812009.
- [97] Y. Fukuda et al., “Measurement of the solar neutrino energy spectrum using neutrino electron scattering”, *Phys. Rev. Lett.*, 82, 2430–2434, 1999, hep-ex/9812011.
- [98] C. Giunti, M. C. Gonzalez-Garcia, and C. Pena-Garay, “Four-neutrino oscillation solutions of the solar neutrino problem”, *Phys. Rev.*, D62, 013005, 2000, hep-ph/0001101.
- [99] M. Gonzalez-Garcia and Y. Nir, “Neutrino Masses and Mixing: Evidence and Implications”, 2002, hep-ph/0202058.
- [100] V. N. Gribov and B. Pontecorvo, “Neutrino astronomy and lepton charge”, *Phys. Lett.*, B28, 493, 1969.
- [101] D. E. Groom et al., “Review of particle physics”, *Eur. Phys. J.*, C15, 1, 2000, <http://pdg.lbl.gov>.
- [102] A. H. Guth, L. Randall, and M. Serna, “Day-night and energy variations for maximal neutrino mixing angles”, *JHEP*, 08, 018, 1999, hep-ph/9903464.
- [103] M. M. Guzzo, A. Masiero, and S. T. Petcov, “On the MSW effect with massless neutrinos and no mixing in the vacuum”, *Phys. Lett.*, B260, 154–160, 1991.
- [104] M. M. Guzzo and S. T. Petcov, “On the matter enhanced transitions of solar neutrinos in the absence of neutrino mixing in vacuum”, *Phys. Lett.*, B271, 172–178, 1991.
- [105] W. Hampel et al., “GALLEX solar neutrino observations: Results for GALLEX III.”, *Phys. Lett.*, B388, 384–396, 1996.
- [106] W. Hampel et al., “Final results of the Cr-51 neutrino source experiments in GALLEX”, *Phys. Lett.*, B420, 114–126, 1998.
- [107] W. Hampel et al., “Verification tests of the GALLEX solar neutrino detector, with Ge-71 produced in-situ from the beta-decay of As-71”, *Phys. Lett.*, B436, 158–173, 1998.
- [108] W. Hampel et al., “GALLEX solar neutrino observations: Results for GALLEX IV”, *Phys. Lett.*, B447, 127–133, 1999.
- [109] W. C. Haxton, “Analytic treatments of matter enhanced solar neutrino oscillations”, *Phys. Rev.*, D35, 2352, 1987.

- [110] K. S. Hirata et al., "Observation of B-8 solar neutrinos in the Kamiokande-II detector", *Phys. Rev. Lett.*, 63, 16, 1989.
- [111] K. S. Hirata et al., "Constraints on neutrino oscillation parameters from the Kamiokande-II solar neutrino data", *Phys. Rev. Lett.*, 65, 1301–1304, 1990.
- [112] K. S. Hirata et al., "Results from one thousand days of real-time, directional solar-neutrino data", *Phys. Rev. Lett.*, 65, 1297–1300, 1990.
- [113] K. S. Hirata et al., "Real time, directional measurement of B-8 solar neutrinos in the Kamiokande-II detector", *Phys. Rev.*, D44, 2241–2260, 1991.
- [114] K. S. Hirata et al., "Search for day / night and semiannual variations in the solar neutrino flux observed in the Kamiokande-II detector", *Phys. Rev. Lett.*, 66, 9–12, 1991.
- [115] H. Nunokawa, W. J. C. Teves, and R. Z. Funchal, "Determining the oscillation parameters by Solar neutrinos and KamLAND", 2002, hep-ph/0212202.
- [116] C. W. Kim and A. Pevsner, *Neutrinos in physics and astrophysics*, Harwood Academic Press, Chur, Switzerland, 1993, Contemporary Concepts in Physics, Vol. 8.
- [117] M. Koshiba, "Observational neutrino astrophysics", *Phys. Rept.*, 220, 229–381, 1992.
- [118] P. I. Krastev and S. T. Petcov, "On the analytic description of two neutrino transitions of solar neutrinos in the sun", *Phys. Lett.*, B207, 64, 1988.
- [119] P. I. Krastev and S. T. Petcov, "Neutrino oscillations in vacuum as a possible solution of the solar neutrino problem", *Phys. Lett.*, B285, 85–90, 1992.
- [120] P. I. Krastev and S. T. Petcov, "Recent solar neutrino observations and unconventional neutrino properties", *Phys. Lett.*, B299, 99–110, 1993.
- [121] T. K. Kuo and J. Pantaleone, "The solar neutrino problem and three neutrino oscillations", *Phys. Rev. Lett.*, 57, 1805–1808, 1986.
- [122] T. K. Kuo and J. Pantaleone, "Three neutrino oscillations and the solar neutrino experiments", *Phys. Rev.*, D35, 3432, 1987.
- [123] T. K. Kuo and J. Pantaleone, "Neutrino oscillations in matter", *Rev. Mod. Phys.*, 61, 937, 1989.
- [124] T. K. Kuo and J. Pantaleone, "Nonadiabatic neutrino oscillations in matter", *Phys. Rev.*, D39, 1930, 1989.
- [125] V. A. Kuzmin, *Zh. Eksp. Teor. Fiz.*, 49, 1532, 1965, [Sov. Phys. JETP 22, 1051 (1966)].
- [126] C.-S. Lim and W. J. Marciano, "Resonant spin-flavor precession of solar and supernova neutrinos", *Phys. Rev.*, D37, 1368, 1988.
- [127] E. Lisi, A. Marrone, D. Montanino, A. Palazzo, and S. T. Petcov, "Analytical description of quasi-vacuum oscillations of solar neutrinos", *Phys. Rev.*, D63, 093002, 2001, hep-ph/0011306.
- [128] E. Lisi and D. Montanino, "Earth regeneration effect in solar neutrino oscillations: An analytic approach", *Phys. Rev.*, D56, 1792–1803, 1997, hep-ph/9702343.

- [129] Q. Y. Liu, M. Maris, and S. T. Petcov, "A study of the day-night effect for the super-Kamiokande detector. I: Time averaged solar neutrino survival probability", *Phys. Rev.*, D56, 5991–6002, 1997, hep-ph/9702361.
- [130] M. Maltoni, T. Schwetz, M. A. Tortola, and J. W. F. Valle, "Constraining neutrino oscillation parameters with current solar and atmospheric data", 2002, hep-ph/0207227.
- [131] M. Maltoni, T. Schwetz, M. A. Tortola, and J. W. F. Valle, "Ruling out four-neutrino oscillation interpretations of the LSND anomaly?", *Nucl. Phys.*, B643, 321–338, 2002, hep-ph/0207157.
- [132] M. Maltoni, T. Schwetz, and J. Valle, "Combining first KamLAND results with solar neutrino data", 2002, hep-ph/0212129.
- [133] S. P. Mikheev and A. Y. Smirnov, "Resonance enhancement of oscillations in matter and solar neutrino spectroscopy", *Sov. J. Nucl. Phys.*, 42, 913–917, 1985.
- [134] S. P. Mikheev and A. Y. Smirnov, "Resonant amplification of neutrino oscillations in matter and solar neutrino spectroscopy", *Nuovo Cim.*, C9, 17–26, 1986.
- [135] S. P. Mikheev and A. Y. Smirnov, "Resonance oscillations of neutrinos in matter", *Sov. Phys. Usp.*, 30, 759–790, 1987.
- [136] L. Miramonti and F. Reseghetti, "Solar neutrino physics: Historical evolution, present status and perspectives", *La Rivista del Nuovo Cimento*, 25, 1, 2002.
- [137] R. N. Mohapatra and P. B. Pal, *Massive neutrinos in physics and astrophysics. Second edition*, volume 60, 1998.
- [138] S. Nakamura, T. Sato, V. Gudkov, and K. Kubodera, "Neutrino reactions on deuteron", *Phys. Rev.*, C63, 034617, 2001, nucl-th/0009012.
- [139] L. B. Okun, "On the electric dipole moment of neutrino", *Sov. J. Nucl. Phys.*, 44, 546, 1986.
- [140] L. B. Okun, M. B. Voloshin, and M. I. Vysotsky, "Electromagnetic properties of neutrino and possible semiannual variation cycle of the solar neutrino flux", *Sov. J. Nucl. Phys.*, 44, 440, 1986.
- [141] L. B. Okun, M. B. Voloshin, and M. I. Vysotsky, "Neutrino electrodynamics and possible consequences for solar neutrinos", *Sov. Phys. JETP*, 64, 446–452, 1986.
- [142] S. J. Parke, "Nonadiabatic level crossing in resonant neutrino oscillations", *Phys. Rev. Lett.*, 57, 1275–1278, 1986.
- [143] M. Passera, "QED corrections to neutrino electron scattering", *Phys. Rev.*, D64, 113002, 2001, hep-ph/0011190.
- [144] S. T. Petcov, "On the nonadiabatic neutrino oscillations in matter", *Phys. Lett.*, B191, 299, 1987.
- [145] S. T. Petcov, "Exact analytic description of two neutrino oscillations in matter with exponentially varying density", *Phys. Lett.*, B200, 373–379, 1988.
- [146] S. T. Petcov, "On the oscillations of solar neutrinos in the sun", *Phys. Lett.*, B214, 139, 1988.
- [147] S. T. Petcov, "Diffractive-like (or parametric-resonance-like?) enhancement of the earth (day-night) effect for solar neutrinos crossing the earth core", *Phys. Lett.*, B434, 321–332, 1998, hep-ph/9805262.

- [148] S. T. Petcov and S. Toshev, "Three neutrino oscillations in matter: analytical results in the adiabatic approximation", *Phys. Lett.*, B187, 120, 1987.
- [149] P. Pizzochero, "Nonadiabatic level crossing in neutrino oscillations for an exponential solar density profile", *Phys. Rev.*, D36, 2293–2296, 1987.
- [150] B. Pontecorvo, 1946, Chalk River Report PD 205.
- [151] B. Pontecorvo, "Neutrino experiments and the question of leptonic-charge conservation", *Sov. Phys. JETP*, 26, 984–988, 1968.
- [152] J. Pulido, "The Solar neutrino problem and the neutrino magnetic moment", *Phys. Rept.*, 211, 167–199, 1992.
- [153] C. E. Rolfs and W. S. Rodney, *Cauldrons in the Cosmos*, The University of Chicago Press, 1988.
- [154] X. Shi and D. N. Schramm, "Solar neutrinos and the MSW effect for three neutrino mixing", *Phys. Lett.*, B283, 305–312, 1992.
- [155] M. B. Smy, "Solar Neutrino Precision Measurements using all 1496 Days of Super-Kamiokande-I Data", 2002, http://neutrino2002.ph.tum.de/pages/transparencies/smy_hep-ex/0208004, XXth International Conference on Neutrino Physics and Astrophysics May 25 - 30, 2002, Munich, Germany.
- [156] A. Strumia, C. Cattadori, N. Ferrari, and F. Vissani, "Which solar neutrino data favour the LMA solution?", *Phys. Lett.*, B541, 327–331, 2002, hep-ph/0205261.
- [157] S. Toshev, "Exact analytical solution of the two neutrino evolution equation in matter with exponentially varying density", *Phys. Lett.*, B196, 170, 1987.
- [158] S. Toshev, "Resonant amplification of three neutrino oscillations in matter", *Phys. Lett.*, B185, 177, 1987.
- [159] Y. Totsuka, "Neutrino astronomy", *Rept. Prog. Phys.*, 55, 377–430, 1992.
- [160] J. W. F. Valle, "Resonant oscillations of massless neutrinos in matter", *Phys. Lett.*, B199, 432, 1987.
- [161] M. B. Voloshin and M. I. Vysotsky, "Neutrino magnetic moment and time variation of solar neutrino flux", *Sov. J. Nucl. Phys.*, 44, 544, 1986.
- [162] L. Wolfenstein, "Neutrino oscillations in matter", *Phys. Rev.*, D17, 2369, 1978.
- [163] G. Wolschin, "Fusion cycles in stars and stellar neutrinos", 2002, astro-ph/0210032.